






Review

Review of Façade Photovoltaic Solutions for Less Energy-Hungry Buildings

Giulio Mangherini ¹, Valentina Diolaiti ^{1,*}, Paolo Bernardoni ², Alfredo Andreoli ¹
and Donato Vincenzi ^{1,3,*}

¹ Department of Physics and Earth Sciences, University of Ferrara, v. G. Saragat 1, 44122 Ferrara, Italy; giulio.mangherini@unife.it (G.M.); alfredo.andreoli@unife.it (A.A.)

² Department of Chemical, Pharmaceutical and Agricultural Sciences, University of Ferrara, v. L. Borsari 46, 44121 Ferrara, Italy; paolo.bernardoni@unife.it

³ Consorzio Futuro in Ricerca, v. G. Saragat 1, 44122 Ferrara, Italy

* Correspondence: valentina.diolaiti@unife.it (V.D.); donato.vincenzi@unife.it (D.V.)

Abstract: Building-integrated photovoltaic technologies have considerable potential for the generation of onsite renewable energy. Despite this, their market penetration is in a relatively embryonic phase with respect to grounded or building-attached solutions, and they have limited commercial application. Their integration into building façades may represent a key asset in meeting the net-zero emissions by 2050 scenario, in particular for high-rise buildings in which the roof-to-façade ratio is unfavorable for the fulfillment of the energy load using only roof photovoltaic technology. Moreover, different façade orientations extend the production time throughout the day, flattening the power generation curve. Because of the present interest in BIPV systems, several researchers have conducted high-quality reviews focused on specific designs. In this work, various photovoltaic technologies and methods used to manufacture façade BIPV devices are reviewed with the aim of presenting researchers with the recent technological advancements and providing an overview of photovoltaic systems designed for different purposes and their applications rather than a detailed analysis of a specific technology. Lastly, future prospects and the limitations of building-integrated photovoltaic devices are presented.



Citation: Mangherini, G.; Diolaiti, V.; Bernardoni, P.; Andreoli, A.; Vincenzi, D. Review of Façade Photovoltaic Solutions for Less Energy-Hungry Buildings. *Energies* **2023**, *16*, 6901. <https://doi.org/10.3390/en16196901>

Academic Editor: Alon Kuperman

Received: 13 August 2023

Revised: 9 September 2023

Accepted: 14 September 2023

Published: 30 September 2023



Copyright: © 2023 by the authors. Licensee MDPI, Basel, Switzerland. This article is an open access article distributed under the terms and conditions of the Creative Commons Attribution (CC BY) license (<https://creativecommons.org/licenses/by/4.0/>).

Keywords: BIPV; solar façades; CdTe; CIGS; DSSC; perovskite; semi-transparent photovoltaics; energy efficiency; glazing; zero-energy buildings

1. Introduction

The need to tackle climate change is leading to an intensified global interest in energy generation based on renewable sources. Compared to other renewable resources, the harvesting of solar irradiance is one of the most widespread, practical, and economical ways to generate energy [1]. Because of the absence of mechanical motion components, the low maintenance costs, and the abundance of solar energy that reaches the Earth's surface every year (1.8×10^{11} MW) [2], photovoltaics (PVs) represent one of the most promising solutions to fulfill the increasing world power consumption. In fact, the improvement in the cell conversion efficiency coupled with the decrease in manufacturing costs allowed for the installation of 1185 GW by the end of 2022 [3]. According to the International Energy Agency's (IEA) "Renewable Energy Market Update" [4], the global solar PV capacity is envisioned to be able to produce almost 1 TW in 2024, which is sufficient to meet the yearly demand of 650 GW by 2030 and the net-zero emissions by 2050 scenario. The commitment to decreasing greenhouse gas (GHG) emissions related to building energy demands, which accounts for 40% of the global energy supply, is leading to the powering of several operations that extend beyond mere electricity production with solar energy, such as ventilation, air conditioning and refrigeration, water desalination, decontamination, and

heating [5,6]. Figure 1 summarizes the possible applications for which a PV façade can be designed.

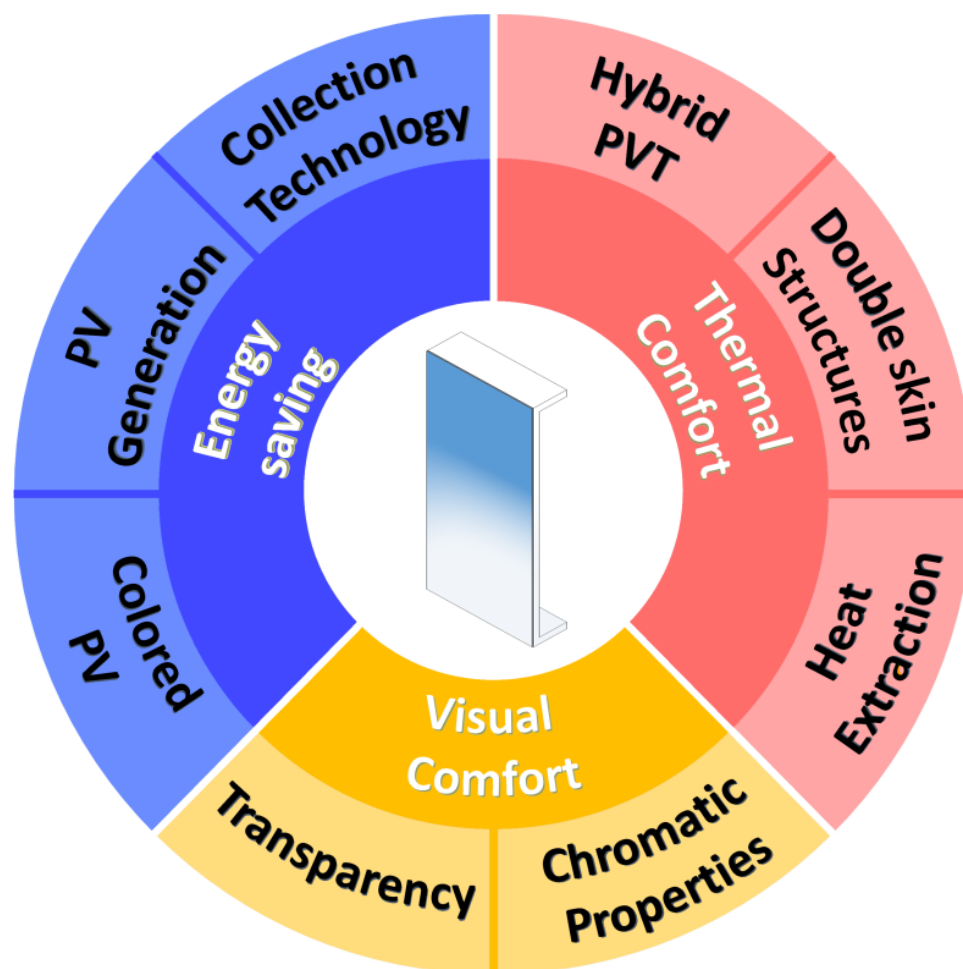


Figure 1. Possible applications and design concepts of PV technologies integrated into building façades.

In particular, buildings' air conditioning and electricity needs consume more than 55% of the global electricity supply, with an estimated annual growth rate of 2.5% [7]. This, coupled with land acquisition constraints and the vast impact that PV plants have on biodiversity and the natural environment, has limited the growth of such plants in favor of smaller-scale distributed installations, especially in urban environments [8,9]. Article 2 of the amended Energy Performance of Buildings Directive (EPBD) (2018/844/EU) [10] aims to support the renovation of the national stock of buildings, residential and non-residential, into highly energy-efficient and decarbonized buildings by 2050, facilitating their transformation towards net-zero energy buildings (NZEBS). Building-integrated photovoltaic (BIPV) technologies constitute interesting and alternative solutions to the production of electricity, eliminating the necessity of areas exclusively dedicated to PV plants [11]. Since BIPV devices directly replace building elements, the surface area for PV installations is provided by the building envelope, and the building's electrical system acts as an interface between the PV panels and the public utility grid [12–14]. Happle et al. [15] established that, if properly installed, BIPVs can limit GHG emissions by up to 50%. This represents a cost-effective method to considerably reduce the environmental impact of a sector that accounts for 39% of total GHG emissions [16].

In this regard, De Boeck et al. [17] identified the increase in a building envelope's insulation efficiency as a key parameter for increasing its energy performance. Furthermore, BIPV technologies are designed to combine power production and insulation efficiency,

improving a building's architectural expression [18]. Indeed, according to IEA Task 15, to actually consider PV modules as building-integrated elements, they must provide additional functions other than energy production, such as mechanical rigidity or structural integrity for the building, impact protection against atmospheric agents (rain, snow, wind, and hail), shading, daylighting, or thermal insulation, as well as fire and noise protection.

A critical issue is represented by glazed surfaces since they highly impact a building's lighting, heating, and ventilation [19]. The design of windows plays an important role in ensuring low cooling and lighting loads for NZEBs [20,21], leading to the implementation of smart windows or dynamic shading systems that increase the resilience of a glazed envelope in terms of energy savings [22,23]. The attention of the scientific community is therefore focused on the study of active glazed surfaces that could improve the building energy demand with respect to conventional static windows, especially for commercial buildings with large transparent façades [24]. De Masi et al. [25] analyzed the impact of windows on building performance in different European climates, showing that, depending on specific factors, such as window typology and orientation, climatic conditions, and window-to-wall ratio, the optimized design of a glazed building envelope may lead to an energy saving varying from 27% to 62%. Similarly, the U.S. Department of Energy reported that window-related energy losses account for up to 25% of a household's energy consumption [26].

A possible solution to further decrease the cost of BIPV technologies is the manufacture of devices that have static or monoaxial concentrating components in the so-called building-integrated concentrating photovoltaic (BICPV) technology. Data from [27–30] estimated that systems with a low-concentration factor specifically designed for building integration can reduce the cost of the device by up to 40% with respect to similar non-concentrating devices. According to the most general definition, a solar concentrator is an object redirecting light rays from a larger area, namely the aperture area, to a smaller one, called the receiver of the absorber area [31]. The ratio between the aperture and the absorber area defines the concentration ratio, which is commonly used to classify optical concentrators. The concentrators enhance the luminous flux that reaches the active PV area by using relatively cheap optical concentrating elements. The goal is to maximize the power generated by the cells by a factor almost equal to the concentration ratio [32], while reducing the amount of PV cells per active area. However, optical concentration also leads to a higher nominal operating cell temperature; therefore, for a medium or high concentration factor, the presence of active cooling procedures is particularly important to avoid limitations in the system efficiency due to additional thermal losses within the PV cells [33,34].

A further strategy to maximize the utilization of solar radiation for building energy efficiency is its concurrent conversion into both thermal and electrical energy via hybrid photovoltaic–thermal (PVT) systems [35,36], also efficiently coupled with BICPVs. Building-integrated photovoltaic–thermal (BIPVT) devices are particularly indicated to support net-zero energy constructions. In addition to their insulation and electricity generation functions, they efficiently harvest a portion of the thermal energy related to solar irradiance [37]. The heat extracted by the thermal collectors of the PVT systems may be used in ventilation air pre-heating [38,39], underfloor heating systems [40], domestic hot water [41], passive and active cooling [42], and heat storage [43,44], thus increasing the overall building energy efficiency.

In terms of architectural and functional design, a façade's optical properties depend on building energy and lighting needs. In Figure 2, an illustration that clarifies the effects of external skin transparency on indoor spaces is presented.

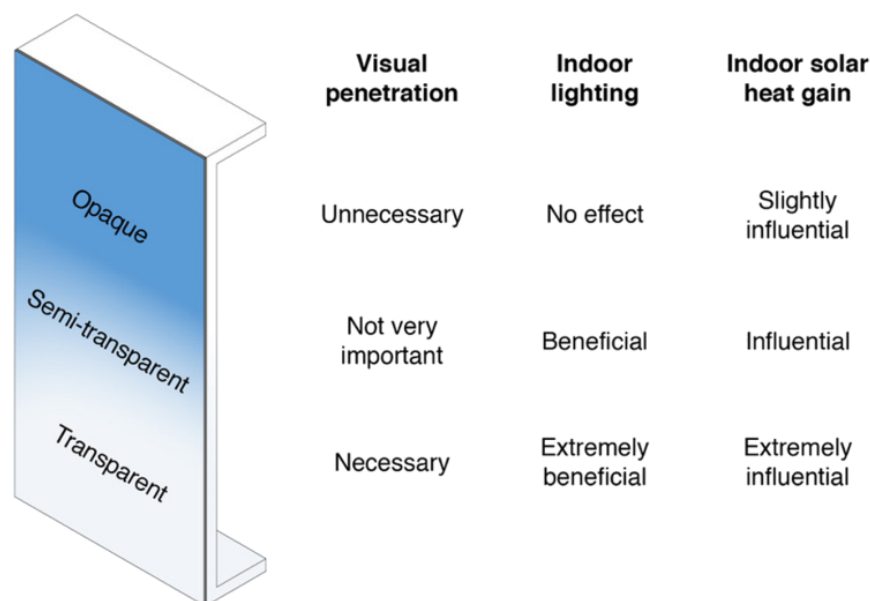


Figure 2. Graphical representation of the external skin transparency effect on the building indoor spaces.

In light of the current surge in interest surrounding BIPV systems, numerous researchers conducted comprehensive reviews that delve into distinct PV technologies. In particular, Sirin et al. [45] reviewed BIPVT systems for green buildings, presenting the operation of these systems, their classification, and potential contributions to building energy efficiency. Several in-depth works on building-integrated and -attached photovoltaic solutions have been performed by A. Ghosh in recent years [46]. In their review on fenestration photovoltaic devices [47], the authors presented different PV-based fenestration-integrated photovoltaic systems to estimate their impact on building energy consumption. Romani et al. [48] further examined this topic by presenting the most common optical, thermal, and electrical models, combined with the modeling capabilities of the most common building simulation tools. In 2022, Massod et al. [49,50] investigated the developments and applications of concentrating photovoltaic technologies. They concluded that the best concentrators for integration in building façades are asymmetric compound parabolic concentrators (ACPCs) and 3D crossed compound parabolic concentrators (CCPCs). Li et al. [51] discussed the recent advances in BIPVs with a particular emphasis on colored technologies, presenting design principles, theoretical analysis, technical routes, and the corresponding demonstration studies. All these works focused on specific PV categories regardless of the building component in which they are integrated. As a further example, Taser et al. [52] provided a comprehensive analysis of BIPV systems, ranging from façade-integrated solutions to roof-mounted solutions. However, due to the breadth of the review, the authors neglected some technical parameters, such as the U-value, the SHGF, or the WWR, which may represent crucial information in the comparison of different PV technologies.

The originality and the main purpose of this article is to provide a review of recent works related to façade-integrated solutions regardless of the technology on which they are based, as a way of providing a compact guide on this topic for readers.

In Section 2, the methodology used to perform this review is described. Section 3 is divided into four sub-sections that provide the most common classification of the PV systems reviewed as well as their working principles. In Section 4, the defined classification is used to describe the contributions of these technologies with the objective of attaining NZEBs, by reporting evidence of their application from the literature. Lastly, in Sections 5 and 6, the discussion and future directions as well as the conclusions of the overall work are reported.

2. Review Methodology

As indicated by the title, this paper focuses on the research and development of photovoltaic technologies integrated into building façades. This review is concerned with the literature published in recent decades and was performed by consulting the relevant databases, such as Scopus, Science Direct, Google Scholar, and Web of Science. The search keywords were BIPV technologies, PV façades, vertically integrated PV panels, colored BIPV, semi-transparent PV devices, integrated PV systems, solar glazing, smart windows, second-generation PV, and third-generation PV. However, due to the wide number of keywords related to this topic, we also employed other terms in order to expand the number of analyzed documents, such as smart, adaptive, advanced, dynamic, and responsive, which were combined with the ones mentioned above. Considering the extension of the analyzed topic, we decided to provide the readers with an overview of the most common design approaches related to vertical BIPV and BIPVT technologies, reviewing both numerical and experimental studies, with particular attention to solutions that have a high technological readiness level. Moreover, since BIPV devices may contribute to attaining NZEBs under different aspects, a higher number of energetic parameters, like thermal and daylighting properties, were considered if present in the investigated documents. In general, BIPV technologies can be organized according to several classifications depending on the review focus. The classification proposed in this paper was based on the PV technology or generation that indicates the active material, the design approach representing the functional capabilities of BIPV systems, and the devices' transparency since this characteristic is independent of other categories, as displayed in Figure 3.

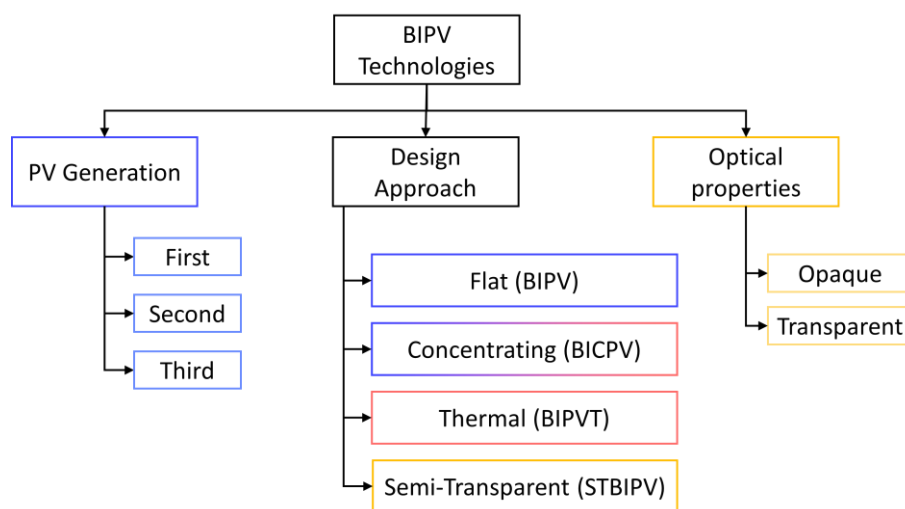


Figure 3. Classification of BIPV technologies.

Table 1 reports the list of acronyms used in this review.

Table 1. List of acronyms used in this work.

Acronyms	Extended Names
PV	Photovoltaic
IEA	International Energy Agency
GHG	Greenhouse Gas
EPBD	Energy Performance of Buildings Directive
NZEB	Net-Zero Energy Building
BIPV	Building-Integrated Photovoltaic
BICPV	Building-Integrated Concentrating Photovoltaic
PVT	Photovoltaic-Thermal
BIPVT	Building-Integrated Photovoltaic-Thermal
ACPC	Asymmetric Compound Parabolic Concentrator

Table 1. Cont.

Acronyms	Extended Names
CCPC	Crossed Compound Parabolic Concentrator
a-Si	Amorphous Silicon
c-Si	Crystalline Silicon
mc-Si	Monocrystalline
pc-Si	Polycrystalline
TF	Thin Film
CIGS	Copper–Indium–Gallium–Selenide
CdTe	Cadmium Telluride
DSSC	Dye-Sensitized Solar Cell
PSC	Perovskite Solar Cell
OPV	Organic Photovoltaic
CPC	Compound Parabolic Concentrator
FR	Fresnel Reflector
LSC	Luminescent Solar Concentrator
STC	Standard Test Conditions
PCM	Phase-Change Material
STBIPV	Semi-Transparent Photovoltaic
CCT	Correlated Color Temperature
CRI	Color-Rendering Index
DGP	Daylight Glare Probability
DGI	Daylight Glare Index
SHGC	Solar Heat with Gain Coefficient
SF	Solar Factor
WICPV	Window-Integrated Concentrating Photovoltaic
WWR	Window-to-Wall Ratio
CAGR	Compound Annual Growth Rate

3. Overview of Different BIPV Typologies

3.1. Standard BIPV Systems

Cutting-edge BIPV solutions allow for the substitution of several envelope components, such as façades, windows, shading elements, or roofs [53]. However, for high-rise commercial or residential buildings, a rooftop PV alone is not sufficient to achieve the NZEB goal, as the building energy demand is greater than the energy produced by the roof PV installation. This forces a large part of the required PV installation to be placed on the façade, namely, a part of the building envelope having a significant architectural value and providing the building with a characteristic appearance and attractiveness. For this reason, innovative BIPV solutions present a tailored design in terms of transparency, color, or texture, thus increasing the building energy efficiency without compromising the façade aesthetics or functionality [54,55]. Moreover, a façade PV has the possibility of exploiting different orientations to guarantee a more uniform energy production during the entire day [56–58].

Biyik et al. [59] presented the advantages of the implementation of BIPV systems in comparison to utility-scale solutions that can be summarized as an increment in PV deployment areas as well as a reduction in building thermal losses and capital costs.

The efficiency of PV modules, currently in the range of 12–23% for commercial devices [2], depends strongly on the panel technology and its working conditions [41]. Depending on the technologies on which they are based, cutting-edge solar modules can have either single or multiple active layers. These layers may perform the proper conversion of solar energy into electrical energy, or improve the absorption of solar radiation in different ranges, thus enhancing the entire device efficiency [60]. A widespread methodology to classify solar cells and PV panels is based on the technology used for solar cell fabrication: each PV module can be subdivided into three main generations strictly related to the amount of contained crystal silicon [61]. The different generations are depicted in Figure 4. The first generation is characterized by the presence of crystalline silicon (c-Si) solar cells [62], which can be subdivided into monocrystalline (mc-Si) [63,64] or polycrystalline (pc-Si) silicon solar cells [65,66]. Standard second-generation PV panels are thin-film (TF) solar cells that present several advantages over first-generation c-Si devices, especially for building integration, having a lower thickness with respect to the first-generation ones. Indeed, the possibility of achieving TF solar cells with a thickness that ranges from a few nanometers

to a few microns opens the possibility to tailor the flexibility, weight, and transparency of these devices according to their function in the building envelope. In addition, as the cell cost accounts for roughly 50% of the total module price [67], if the manufacturing cost of TF technologies competes with first-generation PV solutions, their implementation may lead to a potential cost reduction [68]. For this reason, research activities aiming to improve the efficiency of TF devices based on different technologies, such as copper–indium–gallium–selenide (CIGS) [69,70], cadmium telluride (CdTe) [71,72], or amorphous silicon (a-Si) [73,74], have significantly increased.

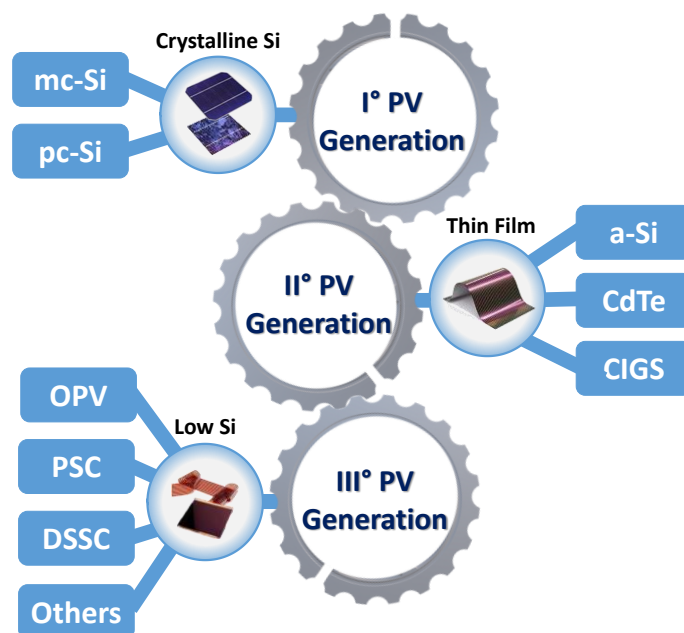


Figure 4. Graphical representation of the three generations of PV technologies.

According to the theoretical Carnot limit, if efficiently converted, solar radiation can generate electricity close to 95% [75]. However, single-junction cells of the first and second generations can only convert 31% due to the Shockley–Queisser limit, whereas third-generation solar cells are free from this limit [76]. The percentage of solar energy not converted into electricity is dissipated as heat. Third-generation solar cells are characterized by devices in which silicon-based solutions play a secondary role and have not yet achieved large-scale manufacturing as opposed to first- and second-generation PVs. Examples of third-generation solar devices are dye-sensitized solar cells (DSSCs) [77,78], perovskite solar cells (PSCs) [79,80], and organic photovoltaics (OPVs) [81,82]. DSSCs include four main components: the photoanode, the counter electrode, the dye sensitizer, and the electrolyte. The first is a wide-bandgap semiconductor that, combined with the dye sensitizer, is needed to actively harvest light, while the electrolyte contains the redox couple for dye regeneration [83]. PSCs are distinguished by perovskite-structured compounds acting as a light-harvesting active layer; the most common ones are hybrid organic–inorganic lead or tin halide-based materials [84]. OPV devices are based on conductive organic polymers or small organic molecules for light absorption and charge transport rather than semiconductor p–n junctions [85]. Despite the technology on which they are based, PV panels are very sensitive to environmental conditions, such as irradiance, dust, humidity, and ambient temperature. Numerous investigations have focused on the influence of the inclination angle and the orientation of PV panels on their performance [86].

3.2. Concentrating BIPV Systems (BICPVs)

The building-integrated concentrating photovoltaic (BICPV) systems represent a niche that is still commercially under-exploited, mainly because of the esthetical constraints

related to the concentrating components. Optical concentrators commonly used in PVT systems can be broadly classified into two main families, namely, conventional and holographic concentrators [87]. These two families can be further subdivided into different types, such as refractive, reflective, hybrid, and luminescent concentrators [88], which can be in turn subdivided into compound parabolic concentrators (CPCs), V-trough reflectors, Fresnel reflectors (FR), or luminescent solar concentrators (LSC) [89–91].

Due to their low transparency, CPCs and V-trough reflectors are preferably employed in low-concentration systems, integrated into opaque roofs or façades [92,93], whereas FR or LSC are usually integrated into transparent or semi-transparent installations [94]. A further advantage of BICPVs is the higher working temperature of the PV cells, since the excess of thermal energy generated on the modules can be used in residential spaces or for water heating, drying and agricultural processes, as well as for other domestic or industrial applications [95,96].

Devices with a concentration ratio greater than $100\times$ are defined as high-concentration systems, and they require both the implementation of high-precision dual-axis tracking and, in some cases, active cooling systems [89]. Systems with a concentration ratio ranging from $10\times$ to $100\times$ are called medium concentration devices, and if their concentration ratio is near $100\times$, they can still feature active cooling but the tracking is limited to a monoaxial one [88]. Objects with a concentration ratio lower than $10\times$ are identified as low-concentration systems that do not require to be coupled with active sun tracking. However, single-axial tracking can be implemented to extend light collection hours during the day [28,97]. The system implemented in BICPV applications are usually medium and low concentrating collectors, as they are stationary or single axial tracking systems [98,99], manufactured to maximize the radiation that reaches the PV cells considering daily and seasonal changes in the solar position [100]. To increase sunlight harvesting, the development of concentrators with a large light acceptance angle is generally preferred to the coupling with a tracking system, as this practice not only decreases the overall system cost but also allows for the concentration of a larger portion of the diffuse radiation.

The ability to focus diffuse radiation makes this type of collector particularly suitable for BICPV applications, as in urban environments diffused contributions can be dominant, especially in high-population-density areas [101,102].

Solar concentrators can be clustered according to the optics, as imaging or non-imaging, or according to their concentration method, since they can be categorized as reflective, refractive, hybrid, or luminescent concentrators [88]. Additionally, CPCs can be subdivided into either two-dimensional or three-dimensional concentrators, depending on whether the concentration is performed on one or two planes [88]. Figure 5 shows the classification of BICVP technologies used in this review.

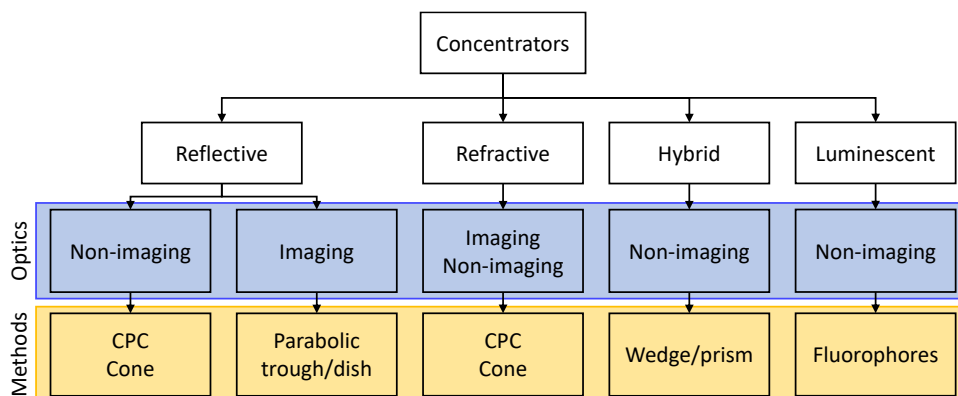


Figure 5. Classification of the concentrating BIPV technologies.

3.3. Photovoltaic–Thermal Systems (BIPVTs)

The electrical power supplied by PV panels depends also on their temperature. In fact, the rating plate of these devices is measured under specific Standard Test Conditions (STCs): irradiance of 1000 W/m^2 , ambient temperature of $25 \text{ }^\circ\text{C}$, and wind speed of 1.5 m/s [103]. Typically, during standard test procedures, the modules are irradiated via flash lamps; thus, the ambient temperature corresponds to the cell temperature, even under STC irradiance. However, in on-field working conditions, if cells are exposed to 1000 W/m^2 , they reach a considerably higher temperature, thus diminishing the power produced by the modules [104,105]. The prolonged increase in the panel surface temperature contributes to an increment in the panel shunt resistance as well as to the creation of hot spots, which not only decrease their performance, but also have an impact on their lifetime. For this reason, the coupling of PV modules with thermal collectors is a widely adopted solution to control the panel overheating, generating the so-called PVT systems. Figure 6 shows the difference between PV and PVT systems and the efficiency increase due to the presence of a thermal collector.

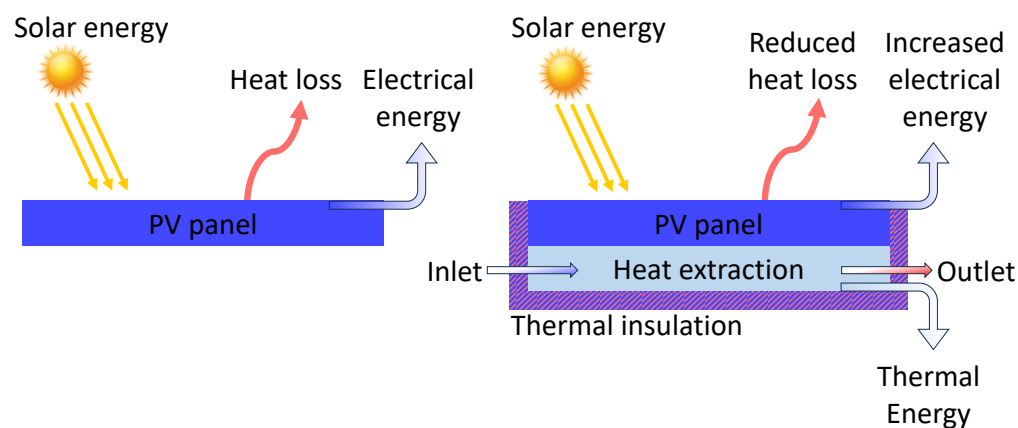


Figure 6. Comparison between the PV and PVT systems' working principles, adapted from [106].

A further advantage of these devices is that the thermal collector is embedded in the system frame and placed behind the PV components, thus employing the same collector area for the extraction of the additional thermal energy. Despite that typical PVT modules are realized for low and medium temperature processes, with a fluid delivery temperature ranging from $20 \text{ }^\circ\text{C}$ to $80 \text{ }^\circ\text{C}$ [107,108], the better efficiency for both thermal and electrical components can only be attained at relatively low temperatures. For ideal operating conditions, the reference temperatures are the ambient temperature and $25 \text{ }^\circ\text{C}$ for the thermal and electrical components, respectively [109,110]. Considering the impact that BIPVT systems may have on NZEBs, various thermal collectors have been developed to enhance the overall system efficiency, such as air [111], water [112], bi-fluidic [113], or thermoelectric [114,115] cooling. Concerning extraction methodology, some of the new developments are nanofluids [116,117], evaporative cooling [118,119], and phase-change material (PCM) [120,121]. As for standard BIPV technologies, BIPVT solutions can be integrated into façades, rooftops, and shading devices [122]; however, in this article, only those related to building façades were analyzed. The classification proposed in this paper is presented in Figure 7.

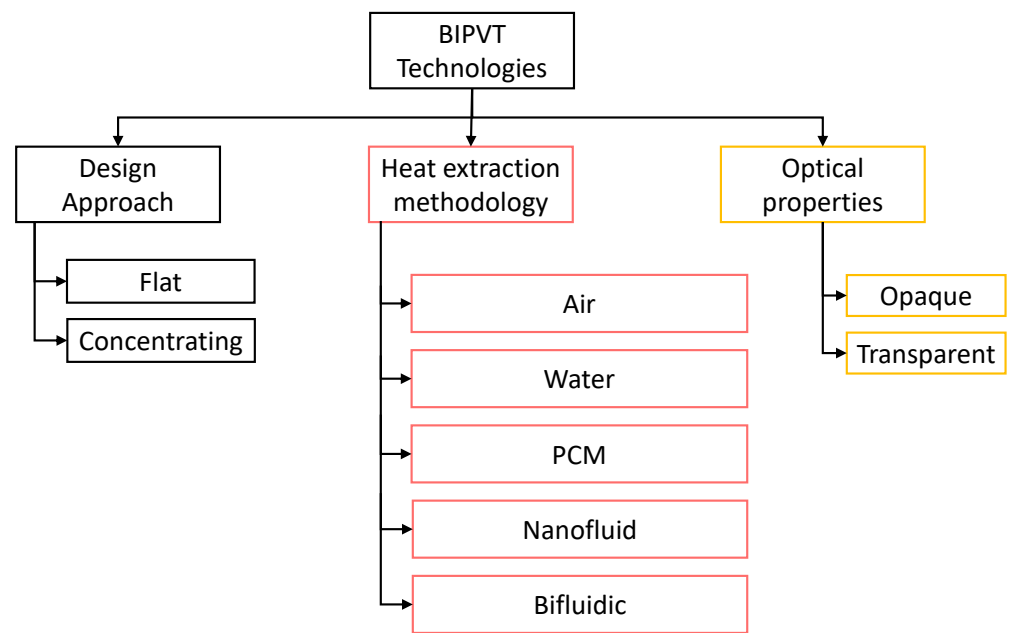


Figure 7. Classification of BIPVT technologies.

3.4. Semi-Transparent Photovoltaic Systems (STBIPVs)

As for opaque BIPV solutions, the absence of mechanical motion components, the low maintenance costs, and the quantity of solar radiation filtering through traditional glazed surfaces into active building elements, make semi-transparent PV technologies the best candidates to turn traditional glazed surfaces into active building elements. In Figure 8, the heat and light transfer phenomena characterizing a standard window are presented. The optimization of fenestration-integrated PV performance is even more delicate with respect to opaque BIPV technologies since the primary purpose of PV windows is the visual and thermal comfort of the building occupants, whereas energy production represents an added value.

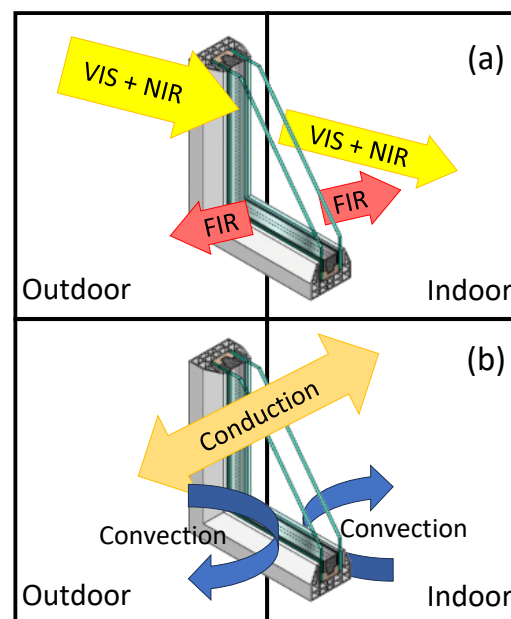


Figure 8. Schematic of a standard window showing (a) the radiative and (b) the conductive and the convective heat transfer mechanisms.

Indeed, as also testified by De Masi et al. [25], for a proper smart window design, additional parameters need to be taken into account, such as transparency, window-to-wall ratio, coverage, fresh air infiltration, and the solar-heat-gain coefficient (SHGC).

The estimation of indoor visual comfort is usually defined by the external daylight penetration [123,124], the correlated color temperature (CCT), and the color rendering index (CRI) [125]. The last two parameters are typically used to define the colorimetric properties of a light source. In this case, the PV glass is assimilated to a light source enlightened by solar radiation and having an emission spectrum equal to its transmission one. To ensure the occupants' visual comfort, the CRI value should be higher than 80 out of 100 and the CCT should range between 3000 K and 7500 K [55]. In the literature, the external daylight that penetrates through fenestration BIPV devices is estimated by using the daylight glare probability (DGP) and the daylight glare index (DGI) [126,127] or by evaluating the illuminance of the building interior, which should be between 100 lx and 2000 lx to avoid discomfort due to glare [128].

All aspects related to thermal comfort are not of secondary importance, namely, the thermal energy transmission coefficient, U-value ($W/(m^2K)$), SHGC, and solar factor (SF). The U-value quantifies the window heat-insulating properties, whereas the SHGC and SF are dimensionless coefficients, respectively, measuring the solar radiation and the energy transmitted to the window. Both the SHGC and SF range from 0 to 1, with 0 indicating a glaze with no transmittance of radiation or energy while 1 represents the full transmittance of the related quantities [129]. Despite having minor differences, the SHGC and SF are used as alternative parameters to evaluate solar penetration through transparent or semi-transparent surfaces.

Typical single-glazed windows have U-values of 3–5 $W/(m^2K)$, which decrease to 2–2.99 $W/(m^2K)$ if double-glazed air-filled windows are considered. This value can be further reduced by manufacturing multiple-layered windows or by increasing the glass thickness [130]. The adoption of multiple-glazed windows also allows the substitution of the air inside the cavity with inert gas, aerogel [131], or vacuum [132]. Due to the manufacturing process involving innovative techniques or materials, and the common utilization of a multilayer structure, which facilitates the PV component integration, smart windows typically have lower U-values when compared to traditional windows. Since a portion of the incoming radiation is absorbed by the integrated solar technology for energy production, the SHGC is usually lower, which is beneficial for hot climates as it decreases the building cooling load, but it negatively impacts the buildings in cold climatic areas. Smart windows can be subdivided into first, second, and third generation, according to the integrated PV technology.

As c-Si absorbs 90.5% of the incident radiation [133], it behaves as an opaque surface and the transparency of first-generation PV fenestration is obtained by spacing two adjacent cells. Semitransparent PV glazing is therefore realized by encapsulating crystalline PV cells between two glasses using standard encapsulant materials like EVA, PVB, or TPO. The transparency of these smart windows may be varied by modifying the glass transmittance or the cell interspacing. Thin-film PV technologies are particularly indicated for the integration in semi-transparent surfaces as they combine the reliability of first-generation PV cells with the possibility of creating devices that have uniform and continuous transparency. DSSCs, PSCs, and OPVs are becoming increasingly popular semi-transparent PV applications compared to those of previous generations due to their tunable transparency and their simpler fabrication processes [134]. Moreover, DSSCs and OPVs are characterized, respectively, by eco-friendly and low-toxicity properties [135].

4. Applications

4.1. Standard BIPV Systems

Due to the electrification process, a considerable increase in green energy production is required. Considering only ground-based electricity generation, a vast land occupation would be needed. Better alternatives, such as the integration of PV panels into buildings,

are a driving force for countries' energy transition [136]. For instance, the Enzian Office in Bolzano (Italy) is mainly covered with PV modules integrated into the building's glass façade. The building uses PV glass (a-Si), which has a nominal peak power between 21% and 10% depending on the data test conditions [137].

Maturi et al. [138] reported the performance of a BIPV façade system installed in an office situated in the city center of Bolzano (Italy). The results were obtained by considering the PV production data, the climatic conditions, and the module temperature for over 6 months. A subsequent simulation study based on typical environmental parameters was used to project the need for the proper ventilation of PV modules to enhance the overall power output.

Eke et al. [139] compared the performance of two PV façades in the Turkish climate. The PV coverage was 405 m² for a total installed power capacity of 40.3 kWp. The modules were based on single- and triple-junction a-Si technology, and the shading effect on the performance of two triple-junction PV systems was analyzed. The system was organized in five PV rows and two identical strings whose energy rating values were compared. The former had one row completely shaded, whereas the latter presented smaller shading. The obtained values differed by 16%, with an annual and monthly average ranging between 10% and 24%, respectively. In winter months, the shading was caused by the trees' line and the difference in energy rating values was less than 1%, whereas, during summer, the sun height led to an energy yield difference of about 15%.

Martín-Chivelet et al. [140] performed a building retrofit case study in which standard PV modules were integrated into a new ventilated façade. The integration of PV devices into the substitution of polymer concrete panels has been very positive, ensuring a self-sufficiency index of 6.6%. The panels were integrated on different building façades: because of shading, the east-oriented ones exhibited a performance ratio below 60%, except for during wintertime. To limit the partial shading effects, the façades were associated with different sub-systems, ensuring an increment of 0.37 MWh per year. In this particular case, dividing the PV generator into three parts increased the PV's overall production. The module rear ventilation led to an annual efficiency increase of 2.5% when compared to the non-ventilated condition.

In Norway, the Powerhouse Brattørkaia is an "energy positive" office building in Trondheim where PV modules were installed on the roof and the upper part of the façade covering an area of 2860 m², producing roughly 458 MWh/year [141]. The building is expected to generate twice as much energy as was required for its construction and will be required for its operation.

In Denmark, the Copenhagen International School has a façade made out of more than 12,000 solar tiles, each with 50 Wp [142]. As reported by Nørgaard and Poder, the building has about 39% of the total electricity consumption covered by the solar cells: the approximate 6000 m² solar cell area corresponds roughly to a 720 kWp capacity. The 70 × 70 cm² sea-green solar panels are angled in four different orientations to create a sequin-like effect [143].

An efficient way to protect indoor environments can be achieved using double-skin façades. As reported by Naddaf and Baper [144], an annual cooling demand reduction between 9 and 14% was observed when DSF was used.

In 2017, Zanetti et al. [145] reported an improvement related to the integration of colored PV modules into large-scale case studies, such as offices, residential, and public buildings. As an example, a building in Basel was retrofitted by installing BIPV panels in both the northern and southern façades for a total of 23 kWp, which covered around 37% of the total building's energy demand. A further case study, in which the BIPV penetration was even more important, was conducted in the Netherlands, where a residential building with 48 apartments was converted into a ZEB, since the PV modules installed on all façades entirely covered the building energy demand. The utilization of colored solar filters covering the cells to increase the module's architectonic value inevitably leads to a reduction in their efficiency with respect to a bare traditional PV module. According to

Saretta et al. [146], for commercially available devices, this reduction corresponds to -4.6% for grey, -6.2% for blue, -5.4% for green, and -10.8% for gold. In Figure 9, some of the retrofits analyzed in this section are presented.



Figure 9. (a) Southwest view of the building after the retrofit, reproduced with copyright permission from [140]. (b) Renovation of a residential building in Zurich, reproduced with copyright permission from [145]. (c) Picture of the BIPV system installed in Bolzano, reproduced with copyright permission from [138].

The main characteristics of the works analyzed in this section are summarized in Table 2.

Table 2. List of the opaque PV modules integrated into building façades.

Authors, Year	PV Technology	Façade Orientation	Research Objective	Location
Eke et al. [139], 2015	Single- and triple-junction a-Si	East West	Shading impact on PV façade	Turkey
Maturi et al. [138], 2010	pc-Si	South–Est South–West	Performance monitoring Simulation projection	Italy
Martín-Chivelet et al. [140], 2018	mc-Si	East South West	Building refurbishment	Spain
Devetakovic et al. [141], 2020	not specified	South	Building refurbishment	Norway
Nørgaard and Pøder [142], 2018	not specified	East South West North	Building refurbishment	Denmark
Zanetti et al. [145], 2017	a-Si	South North	Building refurbishment	Switzerland

4.2. Concentrating BIPV Systems

4.2.1. Opaque BICPVs

The implementation of BICPV systems in opaque building façades opens the possibility of thermally coupling the back of the PV cells with thermal receivers, thus reducing the overheating produced by the photovoltaic process. This configuration allows for the simultaneous generation of electricity and heat, with an increment in the PV conversion efficiency when compared with the configuration without the thermal receiver, due to the cell's lower temperature. If hybrid CPV systems are integrated, limiting glaring effects and combining their heat extraction necessity with the building energy needs, they may constitute interesting alternatives to flat PV devices. In fact, they maximize the solar energy utilization, reducing the semiconductor material for the active area; therefore, several research works concerning building-integrated or -attached configurations are available in the literature [147–149].

In 2001, Huang et al. [150] estimated the performance of an integrated PVT system in which polycrystalline commercial solar cells were coupled to a heat-gathering system. They demonstrated that the integration of the two solar components proficiently increased the energy-saving efficacy of the entire system, when compared to that of a traditional solar water heating system with a PV module having the same dimensions but working individually. Moreover, the obtained results showed that the integration of an optical concentrator increased the temperature of the overall system and that the produced heat could be potentially used in low-to-medium-temperature thermal applications.

In 2015, Li et al. [151] evaluated the performances of a façade-integrated PVT system based on air-gap lens-walled CPCs, having a geometrical concentration ratio of $2.4\times$. The device was designed for installation in a Chinese city and its optical, electrical, and thermal properties were assessed during two typical days of March and May. During the outdoor characterization tests, the concentrator showed a half acceptance angle of 35° and an average optical efficiency of 83.0% only when direct solar irradiation was considered. This value decreased to around 60% when the diffuse irradiance was considered. Water was used as cooling fluid, recirculating between the thermal collector and a storage tank, with a consequential temperature increase. This variation affected the overall system efficiency, which decreased from 65.5%, for a water temperature of 26.6°C , to 47.3%, when the cooling fluid was at 70°C . The overall efficiency values were calculated using the electrical and thermal efficiencies, which were equal to 6.6% and 52% in the first case and to 6% and 35% in the second one, respectively.

Cappelletti et al. [152] designed a PVT for integration on building façades, using a semi-parabolic mirror as a concentrator. The device was equipped with a monoaxial sun tracing system, and a concentration ratio of $20\times$ was achieved by concentrating the solar radiation on a linear focus. An array of monocrystalline PV cells was placed on the device focal line and coupled with a thermal receiver designed for heat recovery. Depending on the building's architectural needs, the device could be horizontally and vertically mounted: a horizontal-mounted single unit of three meters in length produced 120 kWh/year and 500 kWh/year of electrical and thermal energy, respectively. The results of the numerical analysis, developed thanks to the experimental data collected by a mock-up consisting of four semi-parabolic mirrors, showed that vertical mounting resulted in a lower power production of about 30%.

Lu et al. [153] designed and characterized an ACPC for building façade integration. The ACPC was manufactured with a geometric concentration ratio of $2\times$ and acceptance half angles of 0° and 55° , which enable full-year operation in most European climatic conditions. The module was tested under two different irradiances equal to 69 and 280 W/m^2 and the PV output was, respectively, 1.74 and 1.33 times higher compared to the same module without the ACPC. Subsequently, the authors thermally coupled the PV module back with PCM to decrease the cell working temperature. This integration resulted in an increment in the module efficiency greater than 5% when the incident radiation intensity was equal to 280 W/m^2 , and over 10% for a superior solar radiation of 670 W/m^2 . In a sim-

ilar study, Lu et al. [154] investigated the optimization of the PCM heat transfer properties, thanks to the installation of horizontal and vertical aluminum fins, thus proving that both arrangements can improve the module's thermal performance. In particular, during the PCM phase change, the presence of the fins led to a reduction in the PV system temperature to 25 °C and to an increment of over 12% in the module efficiency, when compared to the CPV panel without the PCM under a solar irradiance of 670 W/m².

Rahmanian et al. [155] studied the performance of a heat sink based on PCMs by developing a numerical model that evaluated the system's thermal and electrical performance for both passive and active cooling conditions. To improve the system's thermal conductivity, the PCM was immersed in a nanofluid container in two configurations: single or multi-smaller packs. The passive cooling single-pack configuration was characterized by a decrease in the cell temperature from 96 °C to 78 °C, providing a 12% and 23% increment, respectively, in the electrical and thermal efficiency with respect to the same systems in the absence of PCM. The multi-pack configuration provided the highest thermal energy storage thanks to 97% of the PCM melting. In the active cooling condition, the cell temperature was reduced up to 43 °C with a uniform distribution. The list of the opaque concentrating solutions presented in this section is summarized in Table 3.

Table 3. Summary of the opaque BICPV analyzed in this work.

Authors, Year	Concentrating Technology	PV Technology	Concentration Ratio	Sun Tracking	Research Objective	Location
Li et al. [151], 2015	Air-gap lens-walled CPC	Not specified	2.4×	No	Outdoor characterization testing	China
Cappelletti et al. [152], 2018	semi-parabolic concentrator	mc-Si	20×	Monoaxial	Performance monitoring Simulation projection	Italy
Lu et al. [153], [154], 2018	ACPC	c-Si	2×	No	Experimental characterization Improvement due to PCM integration	Not specified
Rahmanian et al. [155], 2021	Not specified	c-Si	5×	No	Numerical simulations on PCM heat sink design	Not specified

4.2.2. Semitransparent BICPVs

In 2012, Mammo et al. [156] created a CPV system that was suitable for low-concentrating PVs used in façade integration in buildings. The prototype was based on a three-dimensional CCPC system made of 81 single aluminum CCPCs positioned in a 9 × 9 matrix and coupled with as many solar cells as possible. Each truncated CCPC was manufactured with a height of 16.16 mm and with two square surfaces. The aperture had a side of 19 mm, whereas the absorber area was 10 mm. This geometry ensured a concentration ratio equal to 3.61 × and a half acceptance angle of 30°. The prototype showed a 14% maximum electrical conversion efficiency, and the maximum power produced was three times higher than the one of a similar system without the CCPCs.

In 2013, Sellami et al. [157] suggested an innovative idea for a double-glazed window-integrated concentrating photovoltaic (WICPV) system, based on three different geometric properties. The concentrating components were optimized by imposing three constraints: an elliptical and a square shape for the aperture and the receiver area, respectively, and a section having a hyperbolic profile at the end. To preserve the system's transparency and decrease the system's costs, the concentrators were manufactured by using transparent dielectric materials. The criterion for selecting the most promising concentrator profile depends on the trade-off among the highest efficiency, compactness, and the widest acceptance range.

Sabry et al. [158] analyzed the effect of truncation on the performance of a CPC manufactured using acrylic material and having a geometric concentration ratio of 3.2 ×. The low-concentration integrated photovoltaic system, designed for integration on façades or windows, consisted of a linear CPC segment extending across the horizontal direction,

and with the concentrator axis having an angle of 30° with respect to the horizon. The inclination was chosen to correspond to the latitude of most Middle East countries. The overall system was completed by distributing several concentrators along the panes' vertical direction, with their number depending on the pane height. In their work, Sabry et al. compared the performance of a complete CPC with eight different truncations realized by truncating a different percentage of the concentrator side area. As the CPC side area decreased, the number of CPC units for the unit area increased. The optical efficiency and the concentration ratios of the complete and truncated CPCs were calculated at different incidence angles, and all CPC segments performed better for larger incidence angles. The truncation with a side area of about 70% relative to the complete CPC is of particular interest, as it corresponds to the intersection point between the increase in electricity generated and the reduction in the radiation transmitted by the system.

Most of the research studies from the early 2010s focused on optical simulations as testified by the work of Tang and Wang [159] and Li et al. [160].

Tang and Wang [159] designed a novel static asymmetric lens CPC, demonstrating that truncated and air-gap lens-walled CPCs have a large acceptance angle and guarantee a uniform flux distribution for lower incidence angles. Li et al. investigated several representative designs of lens-walled CPCs obtained by varying different parameters, like the geometric concentration ratio, base height, and truncation ratio. The best-performing configurations were chosen to validate the simulation with experimental measurements performed in Nottingham. The results highlighted that the annual performance of lens-walled CPCs improved with respect to the one of the traditional mirror CPCs, as the overall solar radiation harvested by the lens-walled CPCs was higher.

Xuan et al. [161] designed and manufactured an asymmetric lens CPC for integration into a building's south walls, having a unique rotation angle at the bottom that was introduced to optimize its performance. The authors evaluated the device's optical and electrical performance thanks to ray-tracing simulations and an indoor data acquisition campaign. The peak power of the concentrating module was compared to that of a non-concentrating module, resulting in an output value that was 1.74 times higher. Moreover, the concentrator's optical efficiency was larger than 90% for sunlight incidence angles between 0° and 60° , making the module suitable for integration in south building façades.

In another study, Xuan et al. [162] proposed a general optimization strategy for a unitary asymmetric CPC-based concentrator. The structure was designed to be coupled with PVs or PV/thermal modules for integration in the south-facing wall of a building. Based on this asymmetric structure, four kinds of concentrators were evaluated, namely, a mirror concentrator, a lens-mirror concentrator, a dielectric concentrator, and an air-gap-lens-mirror concentrator. The optimization parameter was the annual performance, analyzed by comparing ray-tracing simulations with the experimental data. The developed systems were found to be suitable for installation in south-facing façades in Chinese regions, since most of them have a latitude that ranges between 25° and 45° . Indeed, the structure with dielectric concentrators presented an acceptance angle between 0° and 85° , even before the optimization, whereas the acceptance angle of the lens-mirror and the air-gap-lens-mirror concentrators was improved after the optimization. In any case, the optimization procedure allowed for the expansion of a geometrical concentration ratio that initially was equal to $2.34\times$. The results presented in [162] were due to a previous work of Xuan et al. [163], in which a PV window integrating an ACPC for simultaneous electricity generation and daylight was reported, having a geometric concentration ratio of $2.50\times$. The authors evaluated the optical performance of the system installed in the southern façade of a building considering also the possible shading effects. The optical simulations indicated that the asymmetric concentrator maintained a high optical efficiency even for wide acceptance angles ($10\text{--}85^\circ$). This analysis led to the optimization of the distances between the different concentrator arrays. In fact, the presence of gaps between two subsequent concentrators alleviated the mutual shading and incorporated daylight as a possible feature for the system. Subsequently, Xuan et al. evaluated the illuminance

distribution at the ground floor of a typical office room incorporating the developed PV window, considering 500 W/m^2 as the external irradiance value with several incidence angles. The obtained results testify to the possibility of using the developed BICPV system for domestic applications.

The work presented by Li et al. [164] and Liang et al. [165] show further confirmation that CPCs can be implemented as curtain walls in semi-transparent façades. The former ensured an interesting power generation efficiency in winter, of 26.5%, but a limited transmittance, of 9.1%, when compared to other concentrating technologies. Moreover, it contributed to a more uniform indoor light environment and complied with the requirements of building insulation. This was a photovoltaic thermal technology that presented a significantly lower electrical efficiency, of 4.18%, but an overall energy efficiency above 59.7%.

Technologies that employ transparent or semi-transparent slabs as concentrating components are alternatives to most standard BICPV systems. In this case, the light is concentrated on the solar cell thanks to the total internal reflection by a unique object rather than several separated concentrators. The main advantage of these concentrators is the possibility of designing PV devices that have a tunable transmittance and uniform transparency, as they only depend on the position in which the PV cells used for energy production are placed. An example is provided in the research of Barone et al. [166], in which a smart concentrating photovoltaic glazing module was developed for integration in a transparent façade. It was composed of a $50 \text{ cm} \times 50 \text{ cm}$ double-glazed panel, in which the outside glass was shaped into several concentrators having thin layers of colored photovoltaic cells in their optical focus. Moreover, the concentrating elements were designed to reduce the direct component of the solar radiation transmitted inside the building, thus maximizing both the natural daylight during the winter season and the PV production in summer. This configuration ensured a PV efficiency between 15.5% and 17.2%, while significantly decreasing the loads associated with artificial lighting and building cooling. Panels that use the total internal reflection as the concentrating phenomenon are particularly indicated for integration in metropolitan areas, since they are able to harvest both direct and diffuse radiation and they are extremely tolerant to shading [167,168].

In particular, in LSC panels, the glass or plastic slab is functionalized with fluorescent materials that collect and re-emit a portion of the sunlight that reaches the slab. The coupling of fluorescence and total internal reflection makes them tolerant to the steep shading generated by trees, streetlights, or chimneys, which usually significantly reduces the performance of standard PV systems [169]. A further advantage of LSC panels is their PV conversion efficiency. The fluorophores used for the slab functionalization are responsible for a down-shifting of the wavelengths that cross the slab, which exposes the silicon solar cells to a wavelength range in which their external quantum efficiency is higher [170].

An example is provided by the work of Corrado et al. [171], in which prototypes of windows with front-facing solar cells were evaluated. In the majority of LSC panels designed for building integrations, the PV components are optically coupled with the panel edges. The investigated configurations allowed the cells to harvest both direct solar irradiance and wave-guided radiation emitted from the fluorescent material embedded in the slab. The authors manufactured several prototypes to evaluate different designs by modifying several parameters, such as the slab thickness, the cell width, and their position. A 5% PV cell coverage of the slab main area ensured an increase in power of $2.2\times$, when compared to the bare cells, and a larger power conversion efficiency of 6.8% was achieved, with a coverage of 31%. The design with the lowest price-to-Watt ratio was manufactured by balancing the power gain and efficiency, and it guaranteed an efficiency equal to 3.8% and a power gain of $1.6\times$. Figure 10 presents some examples of the reviewed opaque and semi-transparent BICPV applications.

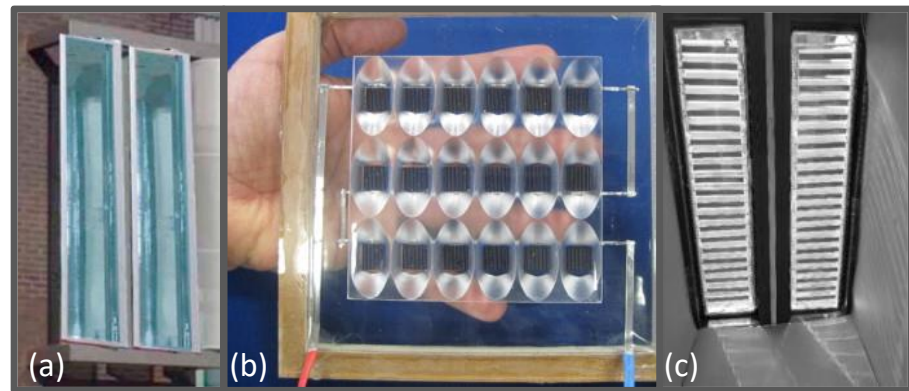


Figure 10. (a) Vertical installation of PVT-integrated devices described in [152] (reproduced with copyright permission). (b) Picture of the window-integrated concentrating photovoltaic system designed in [157] (reproduced with copyright permission). (c) Interior view of the mock-up building realized in [164] (reproduced with copyright permission).

The papers reviewed in this work concerning semi-transparent BICPV solutions are listed in Table 4, which presents the main characteristics of each work.

Table 4. Summary of the semi-transparent BICPVs analyzed in this work.

Authors, Year	Concentrating Technology	PV Technology	Concentration Ratio	Sun Tracking	Research Objective	Location
Mammo et al. [156], 2012	3D CCPC	Not specified	3.61×	No	Performance analysis	Not specified
Sellami et al. [157], 2013	3D CPC	Si	4×	No	Optical characterization and optimization	Not specified
Sabry et al. [158], 2013	Linear CPC	Not specified	3.2×	No	Effect of truncation on the concentrator performance	Location with a latitude of 30°
Tang and Wang [159], 2013	Air-gap lens-walled CPC	Not specified	Not specified	No	Effect of truncation on the concentrator performance	Different locations
Xuan et al. [161], 2017; [163], 2019	Asymmetric lens CPC	mc-Si	2.50×	No	Effect of rotation angle on the concentrator performance	Not specified
Li et al. [164], 2021	ACPC	c-Si	2.0×	No	Experiment performance evaluation	China
Liang et al. [165], 2022	Linear CPC	Not specified	3.14×	Monoaxial	Design and performance validation	China
Barone et al. [166], 2022	Concentrating lens	pc-Si	Not specified	No	Design and performance validation	Multiple locations
Corrado et al. [171], 2013	LSC	mc-Si	Configuration-dependent	No	Design and performance validation	Not specified

4.3. BIPVT Systems

Buonomano et al. [172] presented a detailed exergetic and technoeconomic analysis of a flat-plate PVT solar collector integrated into the south façade of a non-residential high-rise building. The building behavior was modeled via TRNSYS 17 and then compared with a reference building model for three thermal zones. The average exergetic efficiency of the electricity storage system was about 90%, whereas the condensing boiler one was close to 2%. In addition, the economic viability of the proposed system resulted in a simple payback

period of about 4 years. The comparison of the analyzed European weather zones highlighted that the highest destroyed exergy of BIPVTs occurred in Larnaca (150 MWh/year), while the lowest was recorded in Belfast (87 MWh/year). The BIPVT collectors' exergetic efficiencies range from 8.4% for Larnaca to 8.8% for Belfast.

Novelli et al. [173] designed a prototype of a transparent, concentrating photovoltaic thermal system using the direct irradiance for electricity generation and thermal energy. The system was implemented as the interior layer of a façade and it was demonstrated that, in small-scale testing, a cogeneration efficiency of 43.6% (relative to direct normal irradiance transmitted through the building's exterior glazing) at 58 °C could be achieved. Considering a working temperature of 70 °C, which could supply active thermal processes at nominal coefficients of performance, the efficiency decreased to 39.0%. The diffuse light was instead transmitted as illumination and views. By simulating the project scale-up, the cogeneration efficiency increased to 71.2% at 70 °C.

Pugsley et al. [174] described the realization of a façade BIPVT system prototype composed of a PV panel coupled with a solar water heating system. The work demonstrated the practical operation of a vertical BIPVT prototype based on planar liquid–vapor thermal diodes and integrated collector–storage solar water heaters. The key areas for the design development were identified and the benefits of application in NZEB façades were highlighted. The device was subjected to multi-day solar simulator laboratory thermal and photovoltaic testing for different irradiance levels, in both covered and uncovered configurations. The measured solar thermal performance values were 60% and 58% for the cover and uncovered configurations, respectively. As expected, the PV conversion efficiency decreased with the temperature: without the transparent cover, it ranged from 11.4%, when the absorber temperature was about 25 °C, to 5.6%, at 89 °C. The low PV conversion efficiency was due to partial delamination and PV cell damage.

In 2022, Ge et al. [113] proposed a BIPVT system based on water-cooled walls, in which the water-based heat exchanger was not in direct contact with the PV module, as air was used as the intermediate dissipation fluid. The air used to control the overheating of the PV module was, in turn, used to provide hot water or hot air according to the building's needs. The paper experimentally investigated the system's thermo-electrical efficiency, showing an average power generation efficiency equal to 12.6% and providing 35 °C of domestic hot water for more than 7 h.

Pereira and Aelenei [175] installed, in an office building façade, a BIPVT system coupled with PCMs, whose performance was optimized by using the genetic algorithm method. The system was designed starting from a mathematical model, developed with MATLAB/SIMULINK, which was then validated via experimental measurements. The overall energy efficiency of the system was evaluated for winter and summer conditions, adopting different utilization strategies. The parameter optimization allowed a maximum total yield of 64% for the winter configuration and 32% for the summer one.

Sohani et al. [176] enhanced the thermal energy storage capacity of a BIPVT system by employing PCM layers, whose thickness was found using dynamic multi-objective optimization. The optimization was conducted for a residential building in Tehran, Iran, by employing numerical modeling for the system simulation and was based on energetic, economic, and environmental perspectives. According to the simulation results, the best PCM thickness was 0.772 m. This condition was compared to a base case, in which air was used as a heat sink. The implementation of PCM allowed for an increase in the energy storage capacity of 22.24% and the electricity production of 9.93% as well as to reduce the carbon dioxide emission of 17.69%. Moreover, in the optimum conditions, the payback period was estimated to be 3.321 years, with a levelized cost of electricity that was decreased by 9.59%.

Kim et al. [177] assessed the performance of an air-based BIPVT designed for a building façade having in-channel perforated baffle plates as collectors through indoor and outdoor measurements. The indoor thermal characterization was conducted in both open-loop and closed-loop conditions. The former revealed a thermal efficiency between 18% and 42%,

which corresponded to an airflow rate from 85 to 350 kg/h. Under closed-loop conditions, the outdoor measurements provided thermal efficiencies between 12% and 39% with a flow rate varying between 117 and 234 kg/h.

Trombe wall structures are BIPVT systems that are becoming increasingly popular. They are the most popular double-skin structures used to improve the thermal performance in buildings [178,179]. Different configurations between these passive solar heating structures and PVT technologies can be arranged in order to decrease both thermal and electrical building energy needs. Ke et al. [180] investigated the impact of a PCM layer on the performance of a PV system integrated into a Trombe wall. The PCM layer position was changed to identify the best placement for application in the heating season, and the tested configurations are presented in Figure 11. For warm winter regions, the recommended system configuration was characterized by the PCM layer on the back of the PV absorber. This had the lowest space heating effectiveness that was, however, balanced by the best electrical performance. When the PCM layer was located on the wall's inner surface, the system presented moderate electrical performance and space-heating properties, as well as the best energy-saving potential. This disposition was recommended for severely cold winter regions. Comparable results were obtained also for the configuration having the PCM unit coupled to the insulating material. In conclusion, it was found that the performance of the first configuration was the most affected by the PCM layer thickness. Similar innovative applications integrating PV Trombe walls and additional thermal heat sink applications for performance enhancement, such as nanofluids [181] and porous surfaces [182], are present in the literature.

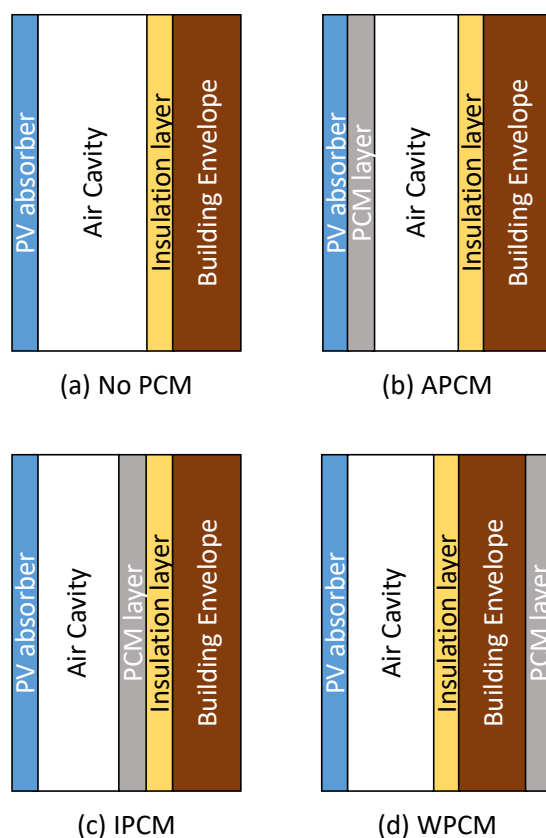


Figure 11. Configurations tested in [180]: (a) without PCM, (b) with the PCM layer next to the absorber back surface, (c) with the PCM placed close to the insulation layer, and (d) with the PCM in contact with the building wall inner surface.

The list of the hybrid PV solutions reviewed in this work, as well as their main features, is presented in Table 5.

Table 5. Summary of the BIPVT analyzed in this work.

Authors, Year	PV Technology	Design Approach	Cooling Fluid	Circulation Technique	Research Objective	Location
Buonomano et al. [172], 2019	Not specified	Flat	Water	Forced	Exergy and thermo-economic modeling	Multiple locations
Novelli et al. [173], 2021	Triple-junction cell	Concentrating	Air	Forced	Performance investigation	United States
Pugsley et al. [174], 2020	mc-Si	Flat	Water	Forced	Physical realization and laboratory testing	Not specified
Ge et al. [113], 2022	CIGS	Flat	Bi-fluidic	Forced	Performance investigation	China
Sohani et al. [176], 2022	Si	Flat	Air	Forced	Multi-objective performance optimization	Iran
Kim et al. [177], 2022	mc-Si	Flat	Air	Natural	Performance assessment	Canada
Ke et al. [180], 2023	mc-Si	Flat	Air/PCM	Natural	Effects of the PCM layer's position on the BIPVT system	China

4.4. Semi-Transparent BIPV Systems

Park et al. [183] analyzed the thermal and electrical properties of several porch-integrated semi-transparent glass–glass modules, in which the back glass was of different colors, namely, clear, colored, or reflective. Moreover, to ensure a higher thermal resistance, the panels were equipped with a further rear glass separated from the colored one thanks to specific spacers. The panel's performance was evaluated both under STC and on-field conditions, highlighting that the rear pane difference affected the amount of daylight and heat gained by indoor spaces as well as the module's electrical performance. This study also investigated the influence of the temperature on the module power production, showing that, when exposed to STC, except for the temperature, the power produced by the modules decreased by about 0.48%/°C, a reduction that increased by 0.52%/°C in the outdoor tests.

Lu et al. [184] simulated the energy performance of semi-transparent single-glazing integrating c-Si PV cells for a typical office in Hong Kong. To consider the overall energy performance in terms of electricity benefits, they converted the total heat gain from semi-transparent BIPV modules into the electricity consumption of water-cooled and air-cooled air-conditioning systems. Examining the impact of the BIPV system for different orientations, they proved that energy saving due to conditioning systems plays a primary role, while the reduction in electricity consumption due to artificial lighting is secondary. The estimated overall electricity benefits were about 900 kWh/year and 1300 kWh/year for water-cooled and air-cooled air-conditioning systems, respectively.

In 2005, Miyazaki et al. [185] simulated the implementation of an a-Si-based smart window in a standard office building in Japan with Energy Plus. According to the study, a 40% transparency and 50% window-to-wall ratio (WWR) represented the optimum combination, ensuring that the electricity consumption was halved (55% reduction) when compared to the single-glazed window with a WWR of 30% and no lighting control.

He et al. [186] compared the thermal performance of a double-layer PV glass with a single-glazed smart window, showing an indoor heat gain reduction of 46.5% and a power-to-conversion efficiency of 3.65% (standard conditions).

Liao and Xu [187] investigated the energy performance of 20% and 32% transparent, single-glass a-S PV fenestration, proving that they positively impacted the building cooling load when compared to both 87% and 71% transparent single and double glazing. However,

they underperformed with respect to 62% low-emissivity, coated double glazing because of the control over NIR transmission.

Chae et al. [188] investigated the energy performance of an office building after the implementation of a-Si-based double-pane windows with different transmittance values. The analyses were performed for six different climatic conditions in the USA, and the test building had 10,000 m² and 652 m² of floor and window areas, respectively, with 30% WWR. Two different solar cell typologies were used: one had a 180 nm textured a-Si absorber as the PV active material, showing a 6% visible transmissivity, whereas the other had a flat a-Si component with different absorber properties. Using the non-textured sample, two devices with 120 nm and 180 nm in thickness and 30% and 14% in transparency were manufactured. The work demonstrated that all the BIPV solutions reduced the building consumption in terms of the annual HVAC system's energy savings for most of the low-latitude locations. In particular, the PV glaze based on the textured morphology saved 34% and 66% of the annual cooling and heating energy, respectively, when compared to a double-layer clear glass window [188].

In 2016, Zhang et al. [189] studied the net energy performance of a-Si PV fenestration integrated into an office room with a WWR of 0.41 by using the Energy Plus software. The dimensions of the simulated building were 2.3 m × 3.0 m × 2.5 m, and the performance of the semi-transparent PV panel (15% visible transmittance) was compared to that of clear single glazing, double-pane glazing, and low-E glazing. In addition to the SHGC, the solar and visible transmittance, and the pane thickness, the authors also reported the U-values of the different systems. The simulations proved that, in Hong Kong, South–West was the best orientation for electricity production, whereas the South guaranteed the best results in terms of overall energy performance. The total energy saving was evaluated based on the simulated energy uses of the air-conditioning and the artificial lighting of the room, and the a-Si smart window saved up to 18%, 16%, and 1% compared to clear single glazing, double-pane glazing, and low-E glazing, respectively.

Chow et al. conducted multiple studies [41,190] concerning double-glazed ventilated PV windows. The basic structure was composed of a semi-transparent a-Si PV and a glass acting as the external and internal panes, respectively, and in between an air ventilation cavity was left. Air circulation was ensured thanks to two louvers being installed above and below the PV modules. This design represents an example of a cooled PV device, as the air entering from the bottom opening reduced the module overheating, cooling the entire cavity, and exiting from the top aperture due to the stack effect. Therefore, the air buoyancy both reduces the building cooling load and the cells' operating temperature, thus increasing their PV conversion efficiency. The authors used Energy Plus to simulate the thermal and optical properties of the systems by using the meteorological weather data of Hong Kong. The results showed that a PV pane transmittance between 0.45 and 0.55 guaranteed the best power production and reduced up to 55% of the building energy needs.

Barman et al. [191] evaluated the integration of smart windows based on CdTe. The device's opto-thermal characteristics were analyzed using both experimental and simulation data. The system was composed of a double-pane structure, with the CdTe TF as the external layer and a low-E glass as the internal one. The comparison of PV glass with different transmittances in the visible range was conducted, specifically, 7.0%, 12.3%, 17.7%, 25.2%, and 32.7%, but maintaining an identical U-value of 1.812 W/m²K allowed the comparison between several SHGC levels. The increase in the TF transmittance considerably impacted the building heating load and the window energy production; at the same time, the increase in cooling loads was moderate. As expected, the annual energy generation was the highest when the devices were South-oriented, with a maximum of 119.6 kWh/m²/year, ensuring the covering of the artificial lighting energy demand, with a 20% WWR. Compared to the reference window, the savings in net energy consumption was 60.4%.

In 2018, Meng et al. [192] simulated the performance of a PV fenestration based on CdTe. The research was performed using Energy Plus as simulation software, considering an installation in a 10-story building located in Hong Kong and with a 0.6 WWR. The

energy potential was evaluated by comparing the obtained results with the performance of both a-Si PV glazing and a traditional window, presenting a saving increment of 15.5% and 19.6%, respectively.

Alrashidi et al. [193] presented the potential of three 15 cm × 15 cm CdTe-based solar windows with different transmittances, namely, 5.77%, 9.54%, and 12.34%. The prototypes' optical properties were evaluated via indoor spectral characterizations, which highlighted that the module with the highest transmittance was the best candidate for a glazing application as it presented visible transmission values that were 113% and 25% higher with respect to the darkest samples, while the SF only increased by 21% and 7%, respectively.

Regarding third-generation PV technologies, Kang et al. [194] investigated the optical and thermal performance of six DSSCs based on red and green dyes with 7 μm, 9 μm, and 11 μm thick TiO₂. The dimensions of the cells were 10 mm × 10 mm × 4.5 mm, and their average visible transmittance, whose values varied from 6% to 30%, was strongly influenced by the TiO₂ thickness. The sample with a visible transmittance of 27% presented a 0.29 SHGC, which reached a maximum of 0.72 for the glazing with 79% visible transmittance. Similarly, Yoon et al. [195] created four different DSSCs whose visible transparency varied between 20% and 39% by modifying the thickness of the TiO₂ layer. The higher short-circuit current of the cell with thicker semiconductor layers ensured a higher power conversion efficiency. Morini and Corrao [196] investigated the thermo-optical and electrical performance of DSSC-integrated patented glass blocks. The analysis was performed via three different software, allowing the estimation of the device's U-value (3.0 W/(m²K)), the SF (79.7%), and the visible transmittance (79.5%).

Selvaraj et al. [197] proved that a 37% transparent PV fenestration based on DSSC decreased by 21% the disturbing glare with respect to a traditional double-glazed window. This comparison was conducted by considering a clear sunny day in a temperate climate. A further work demonstrated that, despite the reduced visible transmittance, the light transmitted through the device two years after its fabrication led to a CRI enhancement [198].

In 2021, Tong et al. [199] studied perovskite modules with dimensions of 5 cm × 5 cm and 10 cm × 10 cm with efficiencies of 14.55% and 10.25%, respectively. The former performed for 1600 h, maintaining 80% of its standard efficiency, while the latter maintained its 10.25% efficiency for over 1100 h.

Ghosh et al. [200] experimentally and analytically analyzed the properties of a perovskite solar cell to evaluate its performance for a BIPV window application. The device showed a solar and visible transmittance of 20% and 30%, respectively, and a power-to-conversion efficiency of 8.13%. The SF angular dependency was measured, presenting values varying between 0.14 and 0.33. The measured U-value was 5.6 W/m²K.

In 2022, Bhandari et al. [201] investigated how different properties of carbon PSCs designed for BIPV applications may be affected by temperature. Both the transparency and the efficiency presented contained variations in the temperature range from 5 °C to 75 °C, showing an average visible transmittance of around 28.5% and a power conversion efficiency of around 8.25%. The AVT slightly increased above 55 °C in ambient conditions, which was explained by correlating the transmittance with the temperature coefficient and efficiency coefficient of transparency. The measured correlated color temperature (CCT) (>4800 K) and CRI (>80) testified the possibility of perovskites in different climates.

Alrashidi et al. [202] evaluated the thermal performance and energy-saving potential of semi-transparent PV devices based on CdTe by analyzing the panel U-value and SHGC. The result highlighted that, when installed facing in the South–West direction, the glazing with the least transparency reduced 96% of the heating due to solar radiation and 23.2% of the cooling energy with respect to conventional clear glazing.

Figure 12 displays the three generations of PV devices used for semi-transparent applications. The list of the reviewed semi-transparent technologies is provided in Table 6, which also highlights their individual properties.

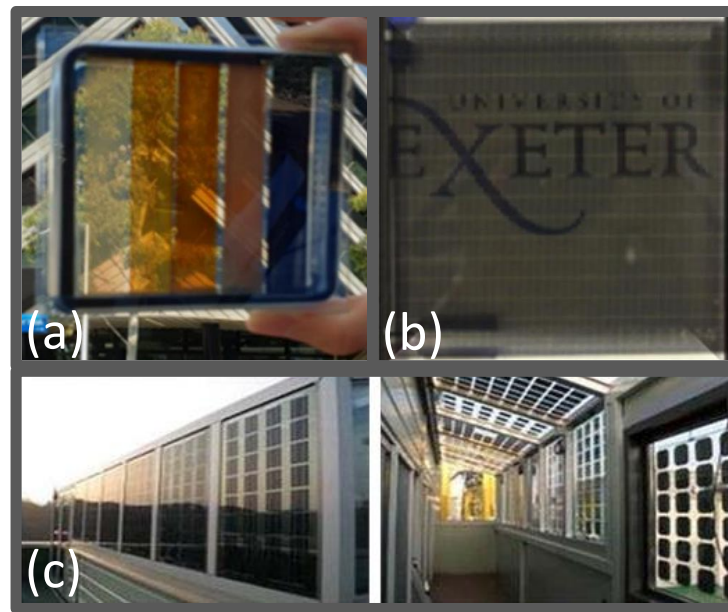


Figure 12. (a) Semi-transparent perovskite solar cells with different transparencies [203]. (b) CdTe-based solar windows with 9.54% transmittance, reproduced with copyright permission from [193]. (c) First-generation glass–glass modules studied in [183] (reproduced with copyright permission).

Table 6. Summary of the STBIPVs analyzed in this work.

Authors, Year	PV Technology	SHGC/SF	WWR	U-value (W/m ² K)	Transmittance	Research Objective	Location
Park et al. [183], 2010	pc-Si	Color-dependent	Not specified	Not specified	Color-dependent	Analysis of the thermal and electrical performance	Korea
Lu et al. [184], 2013	Not specified	Not specified	57%	Not specified	20%	Energy-saving simulations	China
Miyazaki et al. [185], 2005	a-Si	Not specified	50%	Not specified	40%	Energy-saving simulations	Japan
He et al. [186], 2011	a-Si	Not specified	Not specified	Not specified	Not specified	Performance investigation	China
Liao and Xu [187], 2015	a-Si	26% 41%	Configuration-dependent	5.18	20% 32%	Energy performance comparison	China
Chae et al. [188], 2014	a-Si	Configuration-dependent	30%	Configuration-dependent	Configuration-dependent	Performance comparison	Multiple locations
Zhang et al. [189], 2016	a-Si	47%	41%	5.50	15%	Energy performance comparison	China
Barman et al. [191], 2018	CdTe	Configuration-dependent	20–50%	1.81	Configuration-dependent	Efficiency assessment	India
Meng et al. [192], 2018	CdTe	Not specified	60%	Not specified	10%	Performance investigation	China
Kang et al. [194], 2013	DSSC	Configuration-dependent	Not specified	Not specified	Configuration-dependent	Performance evaluation	Not specified
Morini and Corrao [196], 2017	DSSC	Not specified	Not specified	Configuration-dependent	Configuration-dependent	Energy optimization	Not specified
Ghosh et al. [200], 2020	PSC	0.14–0.33	Not specified	5.60	30%	Performance evaluation	Not specified
Alrashidi et al. 2022	CdTe	Configuration-dependent	100%	Configuration-dependent	Configuration-dependent	Thermal and energy performance	Penryn

5. Discussion and Future Perspectives

5.1. Economical Consideration on the Spread of BIPVs

Mainly thanks to its higher stability and durability, when compared to other generations, c-Si covers about 95% of the global PV market, with mc-Si accounting for 84% of the total c-Si production [204]. TF technologies account for the remaining 5%, with CdTe covering the major share (>4%) and CIGS (~0.8%) and a-Si (~0.1) having marginal roles.

Third-generation solar cells do not have, at present, a market share because of their short-term durability when exposed to outdoor ambient conditions (e.g., solar radiation, moisture, and temperature). Although encouraging results have been reported at milder or controlled environmental conditions, to date, they are still far from presenting satisfying stability standards for thin-film PV technology (IEC 61646) and crystalline silicon PV technology (IEC 61215). However, the intrinsic potential of these devices is confirmed by the rapid increase in their energy conversion efficiency [204] and by the compound annual growth rate (CAGR) prevision (2020–2030), which for DSSCs and PSCs is 12.6% and 32%, respectively. The difference in market share is testified also by the price learning curve that shows a reduction between the inflation-adjusted price-to-Watt ratio registered in 2006 3.70 €₂₀₂₁/Wp (TF) 4.78 €₂₀₂₁/Wp (c-Si) and in 2021 0.21 €₂₀₂₁/Wp (TF) 0.18 €₂₀₂₁/Wp (c-Si) [204]. However, due to the presence of multiple business models, different incentives, and application contexts, the BIPV market remains a niche presenting a market share difficult to estimate. In fact, considering opaque façades and glass curtain walls, BIPVs cover different segments with a large variety of products, for which the difference between custom-made and traditional elements can be difficult to assess. As reported by the International Energy Agency in “TRENDS IN PHOTOVOLTAIC APPLICATIONS 2022” [205], even if prices are showing a decrement, BIPV systems present a higher price-to-Watt ratio with respect to both utility-scale ground-mounted PV and distributed rooftops’ PV solutions. In fact, as almost 65% of the PV market is below 1 USD/W, the ratio is almost eight times higher when considering building-integrated PV devices. Metrics used for the competitiveness of BIPV solutions must be considered against additional parameters other than mere power production, such as the replacement of traditional building elements with advanced and better-performing solutions, since PV component integration might be justified by non-economic factors or the perspective of secondary added values.

As reported by SolarPower Europe and ETIP PVs [206], the cost per square meter of PV cladding based on TFs is comparable with that of other materials used in the building sector, such as wood or brick stone, and even if the installation of PV modules based on crystalline silicon is more expensive with respect to these materials, its cost is lower than that of high-standard claddings. Thin-film solar cells are expected to become much cheaper than first-generation solar cells. However, due to the current price decline in wafer-based devices, most thin-film solar cells have not yet become economically viable. Third-generation technologies represent a key asset for the development of BIPV devices with efficiency values that extend beyond that of silicon-based systems. However, up to now, they have a technological readiness level that is too low for their industrial scale-up.

5.2. Future Perspectives

The BIPV market ranges from 200 MW to 400 MW per year in Europe [205]. The proper installation of high-performance and reliable BIPV technologies is correlated to zoning laws and safety regulations. For these reasons, in recent years, BIPV devices have been subjected to wide-ranging research initiatives in which the possibility of improving their performance and reliability was mediated by architectural and safety requirements [207–209]. In that respect, since more expensive systems are often associated with roof-integrated slates, tiles, or tailored designs, the realization of simplified BIPV devices based on conventional PV modules having dedicated mounting structures for building integration is leading the BIPV market towards a positive development in numerous EU countries.

Parallely, several countries are creating regulatory environments promoting direct self-consumption or decentralized or virtual self-consumption. Self-consumption could be

understood as the compensation of production and consumption locally and represents 23% of the distributed PV market. Decentralized (or “Virtual”) self-consumption expands to delocalized production and consumption, enabling the sharing of electricity between several users or between distinct individual buildings.

As highlighted by Skandalos et al. [210], a further aspect that may facilitate the transition to sustainable buildings is the alignment of BIPV technologies with the environmental and architectonic conditions in which they are used. In their work, they analyzed four climatic regions for a total of 127 cities, underlining that, in cold, moderate, and warm climates, opaque-façade BIPV solutions are increasingly indicated to satisfy building energetic needs. PV windows have been reported to be very effective in zones with high and very high solar radiation, as they counterbalance the excess cooling needs. Nonetheless, the implementation of BIPV systems is not yet common due to several factors concerning the lack of proper knowledge in terms of safety and maintenance. Indeed, research initiatives that will enhance the deployment of BIPV technologies are being studied, focusing on properties that extend beyond power production. For instance, it is essential that BIPV implementation does not adversely affect the safety of construction products or building occupants. Fire safety is of vital concern in using these systems. Unfortunately, as reported by Yang et al. [211], although some researchers investigated the fire hazards related to BIPV modules, several knowledge gaps are still present, not only in the mitigation of hazards related to electrical faults but also on BIPV fire resistance or the mitigation of fire spreading. Another limiting factor for the integration of PVs in buildings is soiling due to atmospheric agents [212,213], since dust and snow negatively affect the module power generation. The overcoming of these knowledge gaps represents a crucial step for the further spreading for opaque-façade BIPV solutions, in particular for first-generation devices. Self-cleaning methodologies can represent a considerable asset for the BIPV industry, especially for semi-transparent technologies [214,215]. Correlated to the smart windows concept, there is the possibility of exploiting the electricity generated by the PV component in power-independent appliances and smart systems. A recent example is the device presented by Kou et al. [216], who developed an electrochromic smart window that integrates self-powering, intelligent solar radiation management and energy storage. The creation of multifunctional and standalone PV windows that are able to perform different functions using only the energy produced only by its PV component could allow the overcoming of the limiting factor of these devices, namely, the intrinsic tradeoff between their transparency and efficiency. The localized utilization of the generated electricity represents an additional added value for STBIPV devices as the additional costs related to the connection to the building’s electrical grid will be avoided.

6. Conclusions

In this review, we analyzed the possible applications of PV solutions integrated into building façades, considering the most common designs and use purposes. Façade applications are becoming more frequent due to the necessity of increasing building energy efficiency and enlarging the implementation area. BIPV typologies that are gaining more interest are the ones characterized by the ease of installation and multifunctional behavior, such as hybrid or semi-transparent BIPVs, since they not only replace structural materials, providing electrical power, but also have an impact on the building’s thermal management. The implementation of opaque 1-sun solar panels characterized by dark colors is decreasing in favor of colored PV modules that have hidden cells, which are actively used to preserve the façade’s architectural value, thus guaranteeing the distinctive appearance of the building.

At present, most STBIPV devices are realized and optimized considering only optical properties and power generation. However, the inclusion of standalone appliances or smart systems, such as motorized shading or small ventilation devices, will be a considerable added value for these technologies. For semi-transparent BIPV devices, c-Si-based spaced glazing is still considered an attractive solution due to its maturity and technological

readiness. Nonetheless, second- and third-generation PV-based smart windows should be the leading alternatives in future STBIPV technologies, as their uniform transparency allows for finer control of SHGC, CCT, and CRI, which are essential factors for building windows.

From a broader perspective, the utilization of BIPV solutions is not yet largely implemented because of factors mostly related to technical and political regulations as opposed to the device efficiency, such as missing knowledge related to safety or maintenance.

Author Contributions: Conceptualization, G.M. and V.D.; methodology, G.M. and V.D.; validation, G.M. and V.D.; formal analysis, P.B.; investigation, G.M. and V.D.; resources, D.V.; data curation, G.M. and V.D.; writing—original draft preparation, G.M. and V.D.; writing—review and editing, P.B. and A.A.; visualization, A.A.; supervision, D.V.; project administration, D.V.; funding acquisition, D.V. All authors have read and agreed to the published version of the manuscript.

Funding: This research received no external funding.

Data Availability Statement: No new data were created or analyzed in this study. Data sharing is not applicable to this article.

Conflicts of Interest: The authors declare no conflict of interest.

References

- Dutta, R.; Chanda, K.; Maity, R. Future of Solar Energy Potential in a Changing Climate across the World: A CMIP6 Multi-Model Ensemble Analysis. *Renew. Energy* **2022**, *188*, 819–829. [[CrossRef](#)]
- Maghrabie, H.M.; Abdelkareem, M.A.; Al-Alami, A.H.; Ramadan, M.; Mushtaha, E.; Wilberforce, T.; Olabi, A.G. State-of-the-Art Technologies for Building-Integrated Photovoltaic Systems. *Buildings* **2021**, *11*, 383. [[CrossRef](#)]
- Masson, G.; Bosch, E.; Van Rechem, A.; de l'Epine, M. *Snapshot of Global PV Markets 2023 Task 1 Strategic PV Analysis and Outreach PVPS*; Report IEA-PVPS T1-44:2023; IEA PVPS: Paris, France, 2023; ISBN 978-3-907281-43-7.
- International Energy Agency (IEA). Renewable Energy Market Update Outlook for 2023 and 2024. 2023. Available online: https://iea.blob.core.windows.net/assets/63c14514-6833-4cd8-ac53-f9918c2e4cd9/RenewableEnergyMarketUpdate_June2023.pdf (accessed on 28 July 2023).
- Selimefendigil, F.; Şirin, C. Experimental Investigation of a Parabolic Greenhouse Dryer Improved with Copper Oxide Nano-Enhanced Latent Heat Thermal Energy Storage Unit. *Int. J. Energy Res.* **2021**, *46*, 3647–3662. [[CrossRef](#)]
- Boschetti, M.; Vincenzi, D.; Mangherini, G.; Bernardoni, P.; Andreoli, A.; Gjestila, M.; Camattari, R.; Fugattini, S.; Caramori, S.; Cristino, V.; et al. Modular Stand-Alone Photoelectrocatalytic Reactor for Emergent Contaminant Degradation via Solar Radiation. *Sol. Energy* **2021**, *228*, 120–127. [[CrossRef](#)]
- Maghrabie, H.M.; Elsaid, K.; Sayed, E.T.; Abdelkareem, M.A.; Wilberforce, T.; Olabi, A.G. Building-Integrated Photovoltaic/Thermal (BIPVT) Systems: Applications and Challenges. *Sustain. Energy Technol. Assess.* **2021**, *45*, 101151. [[CrossRef](#)]
- Barron-Gafford, G.A.; Minor, R.L.; Allen, N.A.; Cronin, A.D.; Brooks, A.E.; Pavao-Zuckerman, M.A. The Photovoltaic Heat Island Effect: Larger Solar Power Plants Increase Local Temperatures. *Sci. Rep.* **2016**, *6*, 35070. [[CrossRef](#)]
- Gorman, C.E.; Torsney, A.; Gaughran, A.; McKeon, C.M.; Farrell, C.A.; White, C.; Donohue, I.; Stout, J.C.; Buckley, Y.M. Reconciling Climate Action with the Need for Biodiversity Protection, Restoration and Rehabilitation. *Sci. Total Environ.* **2023**, *857*, 159316. [[CrossRef](#)]
- EUR-Lex Directive (EU) 2018/844 of the European Parliament and of the Council. Available online: https://eur-lex.europa.eu/legal-content/EN/TXT/?uri=uriserv%3AOJ.L_.2018.156.01.0075.01.ENG (accessed on 11 July 2023).
- Zhang, H.; Chen, H.; Liu, H.; Huang, J.; Guo, X.; Li, M. Design and Performance Study of a Low Concentration Photovoltaic-Thermal Module. *Int. J. Energy Res.* **2018**, *42*, 2199–2212. [[CrossRef](#)]
- Dos Santos, Í.P.; Rütther, R. The Potential of Building-Integrated (BIPV) and Building-Applied Photovoltaics (BAPV) in Single-Family, Urban Residences at Low Latitudes in Brazil. *Energy Build.* **2012**, *50*, 290–297. [[CrossRef](#)]
- Parida, B.; Iniyar, S.; Goic, R. A Review of Solar Photovoltaic Technologies. *Renew. Sustain. Energy Rev.* **2011**, *15*, 1625–1636. [[CrossRef](#)]
- Eiffert, P.; Kiss, G.J. *Building-Integrated Photovoltaic Designs for Commercial and Institutional Structures: A Sourcebook for Architects*; DIANE Publishing: Darby, PA, USA, 2000.
- Happle, G.; Shi, Z.; Hsieh, S.; Ong, B.; Fonseca, J.A.; Schlueter, A. Identifying Carbon Emission Reduction Potentials of BIPV in High-Density Cities in Southeast Asia. *J. Phys. Conf. Ser.* **2019**, *1343*, 012077. [[CrossRef](#)]
- Shabunko, V.; Badrinarayanan, S.; Pillai, D.S. Evaluation of In-Situ Thermal Transmittance of Innovative Building Integrated Photovoltaic Modules: Application to Thermal Performance Assessment for Green Mark Certification in the Tropics. *Energy* **2021**, *235*, 121316. [[CrossRef](#)]
- De Boeck, L.; Verbeke, S.; Audenaert, A.; De Mesmaeker, L. Improving the Energy Performance of Residential Buildings: A Literature Review. *Renew. Sustain. Energy Rev.* **2015**, *52*, 960–975. [[CrossRef](#)]

18. Polo López, C.S.; Troia, F.; Nocera, F. Photovoltaic Bipv Systems and Architectural Heritage: New Balance between Conservation and Transformation. an Assessment Method for Heritage Values Compatibility and Energy Benefits of Interventions. *Sustainability* **2021**, *13*, 5107. [[CrossRef](#)]
19. Tavares, P.; Bernardo, H.; Gaspar, A.; Martins, A. Control Criteria of Electrochromic Glasses for Energy Savings in Mediterranean Buildings Refurbishment. *Sol. Energy* **2016**, *134*, 236–250. [[CrossRef](#)]
20. Gratia, E.; De Herde, A. Design of Low Energy Office Buildings. *Energy Build.* **2003**, *35*, 473–491. [[CrossRef](#)]
21. Xing, Y.; Hewitt, N.; Griffiths, P. Zero Carbon Buildings Refurbishment—A Hierarchical Pathway. *Renew. Sustain. Energy Rev.* **2011**, *15*, 3229–3236. [[CrossRef](#)]
22. Carlucci, F.; Negendahl, K.; Fiorito, F. Energy Flexibility of Building Systems in Future Scenarios: Optimization of the Control Strategy of a Dynamic Shading System and Definition of a New Energy Flexibility Metric. *Energy Build.* **2023**, *289*, 113056. [[CrossRef](#)]
23. Hawila, A.A.W.; Merabtine, A.; Troussier, N.; Bennacer, R. Combined Use of Dynamic Building Simulation and Metamodeling to Optimize Glass Facades for Thermal Comfort. *Build. Environ.* **2019**, *157*, 47–63. [[CrossRef](#)]
24. Nageib, A.; Elzafarany, A.M.; Elhefnawy, M.H.; Mohamed, F.O. Using Smart Glazing for Reducing Energy Consumption on Existing Office Building in Hot Dry Climate. *HBRC J.* **2020**, *16*, 157–177. [[CrossRef](#)]
25. De Masi, R.F.; Festa, V.; Gigante, A.; Ruggiero, S.; Peter Vanoli, G. The Role of Windows on Building Performance under Current and Future Weather Conditions of European Climates. *Energy Build.* **2023**, *292*, 113177. [[CrossRef](#)]
26. Feng, Y.; Duan, Q.; Wang, J.; Baur, S. Approximation of Building Window Properties Using in Situ Measurements. *Build. Environ.* **2020**, *169*, 106590. [[CrossRef](#)]
27. Bowden, S.; Wenham, S.R.; Green, M.A. Application of Static Concentrators to Photovoltaic Roof Tiles. *Prog. Photovolt.* **1995**, *3*, 413–423. [[CrossRef](#)]
28. Aldegheri, F.; Baricordi, S.; Bernardoni, P.; Brocato, M.; Calabrese, G.; Guidi, V.; Mondardini, L.; Pozzetti, L.; Tonezzer, M.; Vincenzi, D. Building Integrated Low Concentration Solar System for a Self-Sustainable Mediterranean Villa: The Astonysine House. *Energy Build.* **2014**, *77*, 355–363. [[CrossRef](#)]
29. Vincenzi, D.; Aldegheri, F.; Baricordi, S.; Bernardoni, P.; Calabrese, G.; Guidi, V.; Pozzetti, L. Low Concentration Solar Louvres for Building Integration. *Proc. AIP Conf. Proc.* **2013**, *1556*, 110–113.
30. Mallick, T.K.; Eames, P.C. Design and Fabrication of Low Concentrating Second Generation PRIDE Concentrator. *Sol. Energy Mater. Sol. Cells* **2007**, *91*, 597–608. [[CrossRef](#)]
31. Muhammad-Sukki, F.; Abu-Bakar, S.H.; Ramirez-Iniguez, R.; McMeekin, S.G.; Stewart, B.G.; Sarmah, N.; Mallick, T.K.; Munir, A.B.; Mohd Yasin, S.H.; Abdul Rahim, R. Mirror Symmetrical Dielectric Totally Internally Reflecting Concentrator for Building Integrated Photovoltaic Systems. *Appl. Energy* **2014**, *113*, 32–40. [[CrossRef](#)]
32. Shanks, K.; Senthilarasu, S.; Mallick, T.K. Optics for Concentrating Photovoltaics: Trends, Limits and Opportunities for Materials and Design. *Renew. Sustain. Energy Rev.* **2016**, *60*, 394–407. [[CrossRef](#)]
33. Royne, A.; Dey, C.J.; Mills, D.R. Cooling of Photovoltaic Cells under Concentrated Illumination: A Critical Review. *Sol. Energy Mater. Sol. Cells* **2005**, *86*, 451–483. [[CrossRef](#)]
34. Alharbi, F.H.; Kais, S. Theoretical Limits of Photovoltaics Efficiency and Possible Improvements by Intuitive Approaches Learned from Photosynthesis and Quantum Coherence. *Renew. Sustain. Energy Rev.* **2015**, *43*, 1073–1089. [[CrossRef](#)]
35. Salem Ahmed, M.; Mohamed, A.S.A.; Maghrabie, H.M. Performance Evaluation of Combined Photovoltaic Thermal Water Cooling System for Hot Climate Regions. *J. Sol. Energy Eng. Trans. ASME* **2019**, *141*, 041010. [[CrossRef](#)]
36. Sarhaddi, F.; Farahat, S.; Ajam, H.; Behzadmehr, A.; Mahdavi Adeli, M. An Improved Thermal and Electrical Model for a Solar Photovoltaic Thermal (PV/T) Air Collector. *Appl. Energy* **2010**, *87*, 2328–2339. [[CrossRef](#)]
37. Yu, G.; Yang, H.; Yan, Z.; Kyeredey Ansah, M. A Review of Designs and Performance of Façade-Based Building Integrated Photovoltaic-Thermal (BIPVT) Systems. *Appl. Therm. Eng.* **2021**, *182*, 116081. [[CrossRef](#)]
38. Nagano, K.; Mochida, T.; Shimakura, K.; Murashita, K.; Takeda, S. Development of Thermal-Photovoltaic Hybrid Exterior Wallboards Incorporating PV Cells in and Their Winter Performances. *Sol. Energy Mater. Sol. Cells* **2003**, *77*, 265–282. [[CrossRef](#)]
39. Candanedo, L.M.; Athienitis, A.; Park, K.W. Convective Heat Transfer Coefficients in a Building-Integrated Photovoltaic/Thermal System. *J. Sol. Energy Eng. Trans. ASME* **2011**, *133*, 021002. [[CrossRef](#)]
40. Fraisse, G.; Ménézo, C.; Johannes, K. Energy Performance of Water Hybrid PV/T Collectors Applied to Combisystems of Direct Solar Floor Type. *Sol. Energy* **2007**, *81*, 1426–1438. [[CrossRef](#)]
41. Chow, T.T.; Ji, J.; He, W. Photovoltaic-Thermal Collector System for Domestic Application. *J. Sol. Energy Eng. Trans. ASME* **2007**, *129*, 205–209. [[CrossRef](#)]
42. Oropeza-Perez, I.; Østergaard, P.A. Active and Passive Cooling Methods for Dwellings: A Review. *Renew. Sustain. Energy Rev.* **2018**, *82*, 531–544. [[CrossRef](#)]
43. Reji Kumar, R.; Samykano, M.; Pandey, A.K.; Kadrigama, K.; Tyagi, V.V. Phase Change Materials and Nano-Enhanced Phase Change Materials for Thermal Energy Storage in Photovoltaic Thermal Systems: A Futuristic Approach and Its Technical Challenges. *Renew. Sustain. Energy Rev.* **2020**, *133*, 110341. [[CrossRef](#)]
44. Chow, T.T. A Review on Photovoltaic/Thermal Hybrid Solar Technology. *Appl. Energy* **2010**, *87*, 365–379. [[CrossRef](#)]
45. Şirin, C.; Goggins, J.; Hajdukiewicz, M. A Review on Building-Integrated Photovoltaic/Thermal Systems for Green Buildings. *Appl. Therm. Eng.* **2023**, *229*, 120607. [[CrossRef](#)]

46. Ghosh, A. Potential of Building Integrated and Attached/Applied Photovoltaic (BIPV/BAPV) for Adaptive Less Energy-Hungry Building's Skin: A Comprehensive Review. *J. Clean. Prod.* **2020**, *276*, 123343. [CrossRef]
47. Ghosh, A. Fenestration Integrated BIPV (FIPV): A Review. *Sol. Energy* **2022**, *237*, 213–230. [CrossRef]
48. Romani, J.; Ramos, A.; Salom, J. Review of Transparent and Semi-Transparent Building-Integrated Photovoltaics for Fenestration Application Modeling in Building Simulations. *Energies* **2022**, *15*, 3286. [CrossRef]
49. Masood, F.; Nor, N.B.M.; Nallagownden, P.; Elamvazuthi, I.; Saidur, R.; Alam, M.A.; Akhter, J.; Yusuf, M.; Mehmood, M.; Ali, M. A Review of Recent Developments and Applications of Compound Parabolic Concentrator-Based Hybrid Solar Photovoltaic/Thermal Collectors. *Sustainability* **2022**, *14*, 5529. [CrossRef]
50. Masood, F.; Nor, N.B.M.; Elamvazuthi, I.; Saidur, R.; Alam, M.A.; Akhter, J.; Yusuf, M.; Ali, S.M.; Sattar, M.; Baba, M. The Compound Parabolic Concentrators for Solar Photovoltaic Applications: Opportunities and Challenges. *Energy Rep.* **2022**, *8*, 13558–13584. [CrossRef]
51. Li, Z.; Ma, T.; Yang, H.; Lu, L.; Wang, R. Transparent and Colored Solar Photovoltaics for Building Integration. *Sol. RRL* **2021**, *5*, 2000614. [CrossRef]
52. Taşer, A.; Koyunbaba, B.K.; Kazanasmaz, T. Thermal, Daylight, and Energy Potential of Building-Integrated Photovoltaic (BIPV) Systems: A Comprehensive Review of Effects and Developments. *Sol. Energy* **2023**, *251*, 171–196. [CrossRef]
53. Khencha, K.; Wided, B.R.; Hocine, B. Techno-Economic Study of BIPV in Typical Sahara Region in Algeria. *J. Econ. Dev. Environ. People* **2020**, *9*, 27–59. [CrossRef]
54. Choi, W.J.; Joo, H.J.; Park, J.W.; Kim, S.K.; Lee, J.B. Power Generation Performance of Building-Integrated Photovoltaic Systems in a Zero Energy Building. *Energies* **2019**, *12*, 2471. [CrossRef]
55. Eder, G.; Peharz, G.; Trattnig, R.; Bonomo, P.; Saretta, E.; Frontini, F.; Polo Lopez, C.S.; Rose Wilson, H.; Eisenlohr, J.; Martín Chivelet, N.; et al. COLOURED BIPV Market, Research and Development IEA PVPS Task 15, Report IEA-PVPS T15-07: 2019. 2019. Available online: https://iea-pvps.org/wp-content/uploads/2020/01/IEA-PVPS_15_R07_Coloured_BIPV_report.pdf (accessed on 27 July 2023).
56. Shabunko, V.; Bieri, M.; Reindl, T. Building Integrated Photovoltaic Facades in Singapore: Online BIPV LCC Calculator. In Proceedings of the 2018 IEEE 7th World Conference on Photovoltaic Energy Conversion (WCPEC) (A Joint Conference of 45th IEEE PVSC, 28th PVSEC & 34th EU PVSEC), Waikoloa, HI, USA, 10–15 June 2018; pp. 1231–1233. [CrossRef]
57. Corti, P.; Capannolo, L.; Bonomo, P.; De Berardinis, P.; Frontini, F. Comparative Analysis of BIPV Solutions to Define Energy and Cost-Effectiveness in a Case Study. *Energies* **2020**, *13*, 3827. [CrossRef]
58. Saretta, E.; Caputo, P.; Frontini, F. A Review Study about Energy Renovation of Building Facades with BIPV in Urban Environment. *Sustain. Cities Soc.* **2019**, *44*, 343–355. [CrossRef]
59. Biyik, E.; Araz, M.; Hepbasli, A.; Shahrestani, M.; Yao, R.; Shao, L.; Essah, E.; Oliveira, A.C.; del Caño, T.; Rico, E.; et al. A Key Review of Building Integrated Photovoltaic (BIPV) Systems. *Eng. Sci. Technol. Int. J.* **2017**, *20*, 833–858. [CrossRef]
60. Rabaia, M.K.H.; Abdelkareem, M.A.; Sayed, E.T.; Elsaid, K.; Chae, K.J.; Wilberforce, T.; Olabi, A.G. Environmental Impacts of Solar Energy Systems: A Review. *Sci. Total Environ.* **2021**, *754*, 141989. [CrossRef]
61. Mohammad Bagher, A. Types of Solar Cells and Application. *Am. J. Opt. Photonics* **2015**, *3*, 94. [CrossRef]
62. Radziemska, E. The Effect of Temperature on the Power Drop in Crystalline Silicon Solar Cells. *Renew. Energy* **2003**, *28*, 1–12. [CrossRef]
63. Lämmle, M.; Kroyer, T.; Fortuin, S.; Wiese, M.; Hermann, M. Development and Modelling of Highly-Efficient PVT Collectors with Low-Emissivity Coatings. *Sol. Energy* **2016**, *130*, 161–173. [CrossRef]
64. Sandnes, B.; Rekstad, J. A Photovoltaic/Thermal (PV/T) Collector with a Polymer Absorber Plate. Experimental Study and Analytical Model. *Sol. Energy* **2002**, *72*, 63–73. [CrossRef]
65. Battisti, R.; Corrado, A. Evaluation of Technical Improvements of Photovoltaic Systems through Life Cycle Assessment Methodology. *Energy* **2005**, *30*, 952–967. [CrossRef]
66. Seng, L.Y.; Lalchand, G.; Sow Lin, G.M. Economical, Environmental and Technical Analysis of Building Integrated Photovoltaic Systems in Malaysia. *Energy Policy* **2008**, *36*, 2130–2142. [CrossRef]
67. Madhusudanan, S.P.; Caroline, C.S.; Batabyal, S.K. Sustainable Energy Harvesting Technologies. In *Sulfide and Selenide Based Materials for Emerging Applications*; Dalapati, G., Wong, T.S., Subrata, K., Amit, C., Zhuk, S., Eds.; Elsevier: Amsterdam, The Netherlands, 2022; pp. 15–33. ISBN 9780323998604.
68. Lee, T.D.; Ebong, A.U. A Review of Thin Film Solar Cell Technologies and Challenges. *Renew. Sustain. Energy Rev.* **2017**, *70*, 1286–1297. [CrossRef]
69. Mufti, N.; Amrillah, T.; Taufiq, A.; Sunaryono; Aripriharta; Diantoro, M.; Zulhadjri; Nur, H. Review of CIGS-Based Solar Cells Manufacturing by Structural Engineering. *Sol. Energy* **2020**, *207*, 1146–1157. [CrossRef]
70. Rawat, S.; Gupta, R.; Gohri, S. Performance Assessment of CIGS Solar Cell with Different CIGS Grading Profile. *Mater. Today Proc.* **2023**, *3–6*. [CrossRef]
71. Kumar, N.M. Performance of Single-Sloped Pitched Roof Cadmium Telluride (CdTe) Building-Integrated Photovoltaic System in Tropical Weather Conditions. *Beni-Suef Univ. J. Basic Appl. Sci.* **2019**, *8*, 2. [CrossRef]
72. Alrashidi, H.; Ghosh, A.; Issa, W.; Sellami, N.; Mallick, T.K.; Sundaram, S. Thermal Performance of Semitransparent CdTe BIPV Window at Temperate Climate. *Sol. Energy* **2020**, *195*, 536–543. [CrossRef]

73. Maurus, H.; Schmid, M.; Bliersch, B.; Lechner, P.; Schade, H. PV for BUILDINGS—Benefits and Experiences with Amorphous Silicon in BIPV Applications. *Refocus* **2004**, *5*, 22–27. [[CrossRef](#)]
74. Yoon, J.H.; Song, J.; Lee, S.J. Practical Application of Building Integrated Photovoltaic (BIPV) System Using Transparent Amorphous Silicon Thin-Film PV Module. *Sol. Energy* **2011**, *85*, 723–733. [[CrossRef](#)]
75. Landsberg, P.T.; Badescu, V. Carnot Factor in Solar Cell Efficiencies. *J. Phys. D Appl. Phys.* **2000**, *33*, 3004–3008. [[CrossRef](#)]
76. Dupré, O.; Vaillon, R.; Green, M.A. Physics of the Temperature Coefficients of Solar Cells. *Sol. Energy Mater. Sol. Cells* **2015**, *140*, 92–100. [[CrossRef](#)]
77. Gokul, G.; Pradhan, S.C.; Soman, S. *Dye-Sensitized Solar Cells as Potential Candidate for Indoor/Diffused Light Harvesting Applications: From BIPV to Self-Powered IoTs*; Springer: Singapore, 2019; ISBN 9789811333026.
78. Yuan, H.; Wang, W.; Xu, D.; Xu, Q.; Xie, J.; Chen, X.; Zhang, T.; Xiong, C.; He, Y.; Zhang, Y.; et al. Outdoor Testing and Ageing of Dye-Sensitized Solar Cells for Building Integrated Photovoltaics. *Sol. Energy* **2018**, *165*, 233–239. [[CrossRef](#)]
79. Lim, S.H.; Seok, H.J.; Kwak, M.J.; Choi, D.H.; Kim, S.K.; Kim, D.H.; Kim, H.K. Semi-Transparent Perovskite Solar Cells with Bidirectional Transparent Electrodes. *Nano Energy* **2021**, *82*, 105703. [[CrossRef](#)]
80. Wahad, F.; Abid, Z.; Gulzar, S.; Aslam, M.S.; Rafique, S.; Shahid, M.; Altaf, M.; Ashraf, R.S. Semitransparent Perovskite Solar Cells. In *Fundamentals of Solar Cell Design*; Scrivener Publishing LLC: Beverly, MA, USA, 2023; Chapter 15; pp. 461–503. [[CrossRef](#)]
81. Muteri, V.; Cellura, M.; Curto, D.; Franzitta, V.; Longo, S.; Mistretta, M.; Parisi, M.L. Review on Life Cycle Assessment of Solar Photovoltaic Panels. *Energies* **2020**, *13*, 252. [[CrossRef](#)]
82. Jiang, T.; Zhang, G.; Xia, R.; Huang, J.; Li, X.; Wang, M.; Yip, H.L.; Cao, Y. Semitransparent Organic Solar Cells Based on All-Low-Bandgap Donor and Acceptor Materials and Their Performance Potential. *Mater. Today Energy* **2021**, *21*, 100807. [[CrossRef](#)]
83. Çakar, S.; Özacar, M.; Findik, F. MOFs-Based Dye-Sensitized Photovoltaics. In *Metal-Organic Framework-Based Nanomaterials for Energy Conversion and Storage*; Gupta, R.K., Nguyen, T.A., Yasin, G., Eds.; Elsevier: Amsterdam, The Netherlands, 2022; pp. 487–506. ISBN 9780323911795.
84. Manser, J.S.; Christians, J.A.; Kamat, P.V. Intriguing Optoelectronic Properties of Metal Halide Perovskites. *Chem. Rev.* **2016**, *116*, 12956–13008. [[CrossRef](#)]
85. Ameri, T.; Dennler, G.; Lungenschmied, C.; Brabec, C.J. Organic Tandem Solar Cells: A Review. *Energy Environ. Sci.* **2009**, *2*, 347–363. [[CrossRef](#)]
86. Wu, S.; Xiong, C. Passive Cooling Technology for Photovoltaic Panels for Domestic Houses. *Int. J. Low-Carbon Technol.* **2014**, *9*, 118–126. [[CrossRef](#)]
87. Ferrara, M.A.; Striano, V.; Coppola, G. Volume Holographic Optical Elements as Solar Concentrators: An Overview. *Appl. Sci.* **2019**, *9*, 193. [[CrossRef](#)]
88. Freier, D.; Ramirez-Iniguez, R.; Jafry, T.; Muhammad-Sukki, F.; Gamio, C. A Review of Optical Concentrators for Portable Solar Photovoltaic Systems for Developing Countries. *Renew. Sustain. Energy Rev.* **2018**, *90*, 957–968. [[CrossRef](#)]
89. Chemisana, D. Building Integrated Concentrating Photovoltaics: A Review. *Renew. Sustain. Energy Rev.* **2011**, *15*, 603–611. [[CrossRef](#)]
90. Gite, S.S.; Walke, P.V. Photovoltaic Cell With Concentrating Collector—A Review. *Int. J. Eng. Res. Technol.* **2013**, *2*, 1–8.
91. Mangherini, G.; Bernardoni, P.; Baccaga, E.; Andreoli, A.; Diolaiti, V.; Vincenzi, D. Design of a Ventilated Façade Integrating a Luminescent Solar Concentrator Photovoltaic Panel. *Sustainability* **2023**, *15*, 9146. [[CrossRef](#)]
92. Paul, D.I. Experimental Characterisation of Photovoltaic Modules with Cells Connected in Different Configurations to Address Nonuniform Illumination Effect. *J. Renew. Energy* **2019**, *2019*, 5168259. [[CrossRef](#)]
93. Michael, J.J.; Iqbal, S.M.; Iniyan, S.; Goic, R. Enhanced Electrical Performance in a Solar Photovoltaic Module Using V-Trough Concentrators. *Energy* **2018**, *148*, 605–613. [[CrossRef](#)]
94. Aste, N.; Del Pero, C.; Tagliabue, L.C.; Leonforte, F.; Testa, D.; Fusco, R. Performance Monitoring and Building Integration Assessment of Innovative LSC Components. In Proceedings of the 2015 International Conference on Clean Electrical Power (ICCEP), Taormina, Italy, 16–18 June 2015; pp. 129–133. [[CrossRef](#)]
95. Elsaid, K.; Taha Sayed, E.; Yousef, B.A.A.; Kamal Hussien Rabaia, M.; Ali Abdelkareem, M.; Olabi, A.G. Recent Progress on the Utilization of Waste Heat for Desalination: A Review. *Energy Convers. Manag.* **2020**, *221*, 113105. [[CrossRef](#)]
96. Iqbal, A.; Mahmoud, M.S.; Sayed, E.T.; Elsaid, K.; Abdelkareem, M.A.; Alawadhi, H.; Olabi, A.G. Evaluation of the Nanofluid-Assisted Desalination through Solar Stills in the Last Decade. *J. Environ. Manag.* **2021**, *277*, 111415. [[CrossRef](#)]
97. Tadeu, S.; Rodrigues, C.; Tadeu, A.; Freire, F.; Simões, N. Energy Retrofit of Historic Buildings: Environmental Assessment of Cost-Optimal Solutions. *J. Build. Eng.* **2015**, *4*, 167–176. [[CrossRef](#)]
98. Micheli, L.; Sarmah, N.; Luo, X.; Reddy, K.S.; Mallick, T.K. Opportunities and Challenges in Micro- and Nano-Technologies for Concentrating Photovoltaic Cooling: A Review. *Renew. Sustain. Energy Rev.* **2013**, *20*, 595–610. [[CrossRef](#)]
99. Li, G.; Xuan, Q.; Akram, M.W.; Golizadeh Akhlaghi, Y.; Liu, H.; Shittu, S. Building Integrated Solar Concentrating Systems: A Review. *Appl. Energy* **2020**, *260*, 114288. [[CrossRef](#)]
100. Sarmah, N.; Mallick, T.K. Design, Fabrication and Outdoor Performance Analysis of a Low Concentrating Photovoltaic System. *Sol. Energy* **2015**, *112*, 361–372. [[CrossRef](#)]
101. Pagliaro, M.; Ciriminna, R.; Palmisano, G. BIPV: Merging the Photovoltaic with the Construction Industry. *Prog. Photovolt. Res. Appl.* **2010**, *18*, 61–72. [[CrossRef](#)]

102. Debije, M.G.; Verbunt, P.P.C. Thirty Years of Luminescent Solar Concentrator Research: Solar Energy for the Built Environment. *Adv. Energy Mater.* **2012**, *2*, 12–35. [[CrossRef](#)]
103. Makki, A.; Omer, S.; Sabir, H. Advancements in Hybrid Photovoltaic Systems for Enhanced Solar Cells Performance. *Renew. Sustain. Energy Rev.* **2015**, *41*, 658–684. [[CrossRef](#)]
104. Li, M.; Ji, X.; Li, G.; Wei, S.; Li, Y.F.; Shi, F. Performance Study of Solar Cell Arrays Based on a Trough Concentrating Photovoltaic/Thermal System. *Appl. Energy* **2011**, *88*, 3218–3227. [[CrossRef](#)]
105. Cuce, E.; Cuce, P.M. Improving Thermodynamic Performance Parameters of Silicon Photovoltaic Cells via Air Cooling. *Int. J. Ambient Energy* **2014**, *35*, 193–199. [[CrossRef](#)]
106. Joshi, S.S.; Dhoble, A.S. Photovoltaic-Thermal Systems (PVT): Technology Review and Future Trends. *Renew. Sustain. Energy Rev.* **2018**, *92*, 848–882. [[CrossRef](#)]
107. Mellor, A.; Alonso Alvarez, D.; Guarracino, I.; Ramos, A.; Riverola Lacasta, A.; Ferre Llin, L.; Murrell, A.J.; Paul, D.J.; Chemisana, D.; Markides, C.N.; et al. Roadmap for the Next-Generation of Hybrid Photovoltaic-Thermal Solar Energy Collectors. *Sol. Energy* **2018**, *174*, 386–398. [[CrossRef](#)]
108. Cabral, D. Development and Performance Comparison of a Modified Glazed CPC Hybrid Solar Collector Coupled with a Bifacial PVT Receiver. *Appl. Energy* **2022**, *325*, 119653. [[CrossRef](#)]
109. Bazilian, M.D.; Leenders, F.; Van Der Ree, B.G.C.; Prasad, D. Photovoltaic Cogeneration in the Built Environment. *Sol. Energy* **2001**, *71*, 57–69. [[CrossRef](#)]
110. Bakker, M.; Zondag, H.A.; Elswijk, M.J.; Strootman, K.J.; Jong, M.J.M. Performance and Costs of a Roof-Sized PV/Thermal Array Combined with a Ground Coupled Heat Pump. *Sol. Energy* **2005**, *78*, 331–339. [[CrossRef](#)]
111. Yang, T.; Athienitis, A.K. A Study of Design Options for a Building Integrated Photovoltaic/Thermal (BIPV/T) System with Glazed Air Collector and Multiple Inlets. *Sol. Energy* **2014**, *104*, 82–92. [[CrossRef](#)]
112. Jalalizadeh, M.; Fayaz, R.; Delfani, S.; Mosleh, H.J.; Karami, M. Dynamic Simulation of a Trigeneration System Using an Absorption Cooling System and Building Integrated Photovoltaic Thermal Solar Collectors. *J. Build. Eng.* **2021**, *43*, 102482. [[CrossRef](#)]
113. Ge, M.; Zhao, Y.; Xuan, Z.; Zhao, Y.; Wang, S. Experimental Research on the Performance of BIPV/T System with Water-Cooled Wall. *Energy Rep.* **2022**, *8*, 454–459. [[CrossRef](#)]
114. Kane, A.; Verma, V.; Singh, B. Optimization of Thermoelectric Cooling Technology for an Active Cooling of Photovoltaic Panel. *Renew. Sustain. Energy Rev.* **2017**, *75*, 1295–1305. [[CrossRef](#)]
115. Kosyvakis, D.N.; Voutsinas, G.D.; Hristoforou, E.V. Experimental Analysis and Performance Evaluation of a Tandem Photovoltaic-Thermoelectric Hybrid System. *Energy Convers. Manag.* **2016**, *117*, 490–500. [[CrossRef](#)]
116. Elsaied, K.; Abdelkareem, M.A.; Maghrabie, H.M.; Sayed, E.T.; Wilberforce, T.; Baroutaji, A.; Olabi, A.G. Thermophysical Properties of Graphene-Based Nanofluids. *Int. J. Thermofluids* **2021**, *10*, 100073. [[CrossRef](#)]
117. Maghrabie, H.M.; Elsaied, K.; Sayed, E.T.; Abdelkareem, M.A.; Wilberforce, T.; Ramadan, M.; Olabi, A.G. Intensification of Heat Exchanger Performance Utilizing Nanofluids. *Int. J. Thermofluids* **2021**, *10*, 100071. [[CrossRef](#)]
118. Alami, A.H. Effects of Evaporative Cooling on Efficiency of Photovoltaic Modules. *Energy Convers. Manag.* **2014**, *77*, 668–679. [[CrossRef](#)]
119. Chandrasekar, M.; Senthilkumar, T. Passive Thermal Regulation of Flat PV Modules by Coupling the Mechanisms of Evaporative and Fin Cooling. *Heat Mass Transf.* **2016**, *52*, 1381–1391. [[CrossRef](#)]
120. Pandey, A.K.; Hossain, M.S.; Tyagi, V.V.; Abd Rahim, N.; Selvaraj, J.A.L.; Sari, A. Novel Approaches and Recent Developments on Potential Applications of Phase Change Materials in Solar Energy. *Renew. Sustain. Energy Rev.* **2018**, *82*, 281–323. [[CrossRef](#)]
121. Stropnik, R.; Stritih, U. Increasing the Efficiency of PV Panel with the Use of PCM. *Renew. Energy* **2016**, *97*, 671–679. [[CrossRef](#)]
122. Rezk, H.; AL-Oran, M.; Gomaa, M.R.; Tolba, M.A.; Fathy, A.; Abdelkareem, M.A.; Olabi, A.G.; El-Sayed, A.H.M. A Novel Statistical Performance Evaluation of Most Modern Optimization-Based Global MPPT Techniques for Partially Shaded PV System. *Renew. Sustain. Energy Rev.* **2019**, *115*, 109372. [[CrossRef](#)]
123. Knoop, M.; Stefani, O.; Bueno, B.; Matusiak, B.; Hobday, R.; Wirz-Justice, A.; Martiny, K.; Kantermann, T.; Aarts, M.P.J.; Zemmouri, N.; et al. Daylight: What Makes the Difference? *Light. Res. Technol.* **2020**, *52*, 423–442. [[CrossRef](#)]
124. Quek, G.; Wienold, J.; Khanie, M.S.; Erell, E.; Kaftan, E.; Tzempelikos, A.; Konstantzos, I.; Christoffersen, J.; Kuhn, T.; Andersen, M. Comparing Performance of Discomfort Glare Metrics in High and Low Adaptation Levels. *Build. Environ.* **2021**, *206*, 108335. [[CrossRef](#)]
125. Ghosh, A.; Norton, B. Interior Colour Rendering of Daylight Transmitted through a Suspended Particle Device Switchable Glazing. *Sol. Energy Mater. Sol. Cells* **2017**, *163*, 218–223. [[CrossRef](#)]
126. Wienold, J.; Christoffersen, J. Evaluation Methods and Development of a New Glare Prediction Model for Daylight Environments with the Use of CCD Cameras. *Energy Build.* **2006**, *38*, 743–757. [[CrossRef](#)]
127. Wienold, J.; Iwata, T.; Sarey Khanie, M.; Erell, E.; Kaftan, E.; Rodriguez, R.G.; Yamin Garretton, J.A.; Tzempelikos, T.; Konstantzos, I.; Christoffersen, J.; et al. Cross-Validation and Robustness of Daylight Glare Metrics. *Light. Res. Technol.* **2019**, *51*, 983–1013. [[CrossRef](#)]
128. Nabil, A.; Mardaljevic, J. Useful Daylight Illuminances: A Replacement for Daylight Factors. *Energy Build.* **2006**, *38*, 905–913. [[CrossRef](#)]
129. Tait, D.B. Solar Heat Gain Coefficients for High-Mass Glazing Blocks. *ASHRAE Trans.* **2006**, *112*, 9.

130. Kralj, A.; Drev, M.; Žnidaršič, M.; Černe, B.; Hafner, J.; Jelle, B.P. Investigations of 6-Pane Glazing: Properties and Possibilities. *Energy Build.* **2019**, *190*, 61–68. [CrossRef]
131. Buratti, C.; Belloni, E.; Merli, F.; Zinzi, M. Aerogel Glazing Systems for Building Applications: A Review. *Energy Build.* **2021**, *231*, 110587. [CrossRef]
132. Ghosh, A.; Norton, B.; Duffy, A. Effect of Sky Clearness Index on Transmission of Evacuated (Vacuum) Glazing. *Renew. Energy* **2017**, *105*, 160–166. [CrossRef]
133. Santbergen, R.Å.; Zolingen, R.J.C. Van The Absorption Factor of Crystalline Silicon PV Cells: A Numerical and Experimental Study. *Sol. Energy Mater. Sol. Cells* **2008**, *92*, 432–444. [CrossRef]
134. Bati, A.S.R.; Zhong, Y.L.; Burn, P.L.; Nazeeruddin, M.K.; Shaw, P.E.; Batmunkh, M. Next-Generation Applications for Integrated Perovskite Solar Cells. *Commun. Mater.* **2023**, *4*, 2. [CrossRef]
135. Wang, Y.; Chen, Q.; Liu, Z.; Yu, F.; Su, W.; Cai, Z.; Guan, W.; Li, Y.; Sheng, L.; Qi, Z.; et al. Acidochromic Organic Photovoltaic Integrated Device. *Chem. Eng. J.* **2023**, *452*, 139479. [CrossRef]
136. Mazzer, M.; Moser, D. How Solar Energy Could Power Italy without Using More Land. Available online: <https://www.nature.com/articles/d43978-021-00048-z> (accessed on 28 July 2023).
137. Onyx Solar Group LLC. Technical Guide. Available online: http://onyxsolardownloads.com/docs/ALL-YOU-NEED/Technical_Guide.pdf (accessed on 28 July 2023).
138. Maturi, L.; Sparber, W.; Kofler, B.; Bresciani, W. Analysis and Monitoring Results of a Bipv System in Northern Italy. In Proceedings of the EU PVSEC Proceedings, 25th European Photovoltaic Solar Energy Conference and Exhibition/5th World Conference on Photovoltaic Energy Conversion, Valencia, Spain, 6–10 September 2010; pp. 5131–5134.
139. Eke, R.; Demircan, C. Shading Effect on the Energy Rating of Two Identical PV Systems on a Building Façade. *Sol. Energy* **2015**, *122*, 48–57. [CrossRef]
140. Martín-Chivelet, N.; Gutiérrez, J.C.; Alonso-Abella, M.; Chenlo, F.; Cuenca, J. Building Retrofit with Photovoltaics: Construction and Performance of a BIPV Ventilated Façade. *Energies* **2018**, *11*, 1719. [CrossRef]
141. Devetaković, M.; Djordjević, D.; Radojević, M.; Krstić-Furundžić, A.; Burduhos, B.G.; Martinopoulos, G.; Neagoe, M.; Lobaccaro, G. Photovoltaics on Landmark Buildings with Distinctive Geometries. *Appl. Sci.* **2020**, *10*, 6696. [CrossRef]
142. Nørgaard, P.; Poder, S.H. Perspectives on Solar Power in Dense Urban Areas—With Copenhagen International School as Case Study. *J. Eng.* **2019**, *2019*, 5134–5137. [CrossRef]
143. Geleff, J. How to Create Truly Solar-Powered Architecture. Available online: <https://architizer.com/blog/inspiration/stories/cf-moller-solar-tiles/> (accessed on 3 August 2023).
144. Naddaf, M.S.; Baper, S.Y. The Role of Double-Skin Façade Configurations in Optimizing Building Energy Performance in Erbil City. *Sci. Rep.* **2023**, *13*, 1–18. [CrossRef]
145. Zanetti, I.; Bonomo, P.; Frontini, F.; Saretta, E. Building Integrated Photovoltaics: Product Overview for Solar Building Skins. SUPSI, 2017. Available online: https://www.solaxess.ch/wp-content/uploads/2018/04/Report-2017_SUPSI_SEAC_BIPV.pdf (accessed on 3 August 2023).
146. Saretta, E.; Bonomo, P.; Frontini, F. Active BIPV Glass Façades: Current Trends of Innovation. In Proceedings of the GPD Glass Performance Days 2017—Conference Proceedings GPD Glass Performance Days 2017, Tampere, Finland, 28–30 June 2017; pp. 2–7. Available online: <https://api.semanticscholar.org/CorpusID:116363469> (accessed on 24 July 2023).
147. Preet, S. Water and Phase Change Material Based Photovoltaic Thermal Management Systems: A Review. *Renew. Sustain. Energy Rev.* **2018**, *82*, 791–807. [CrossRef]
148. Michael, J.J.; S, I.; Goic, R. Flat Plate Solar Photovoltaic-Thermal (PV/T) Systems: A Reference Guide. *Renew. Sustain. Energy Rev.* **2015**, *51*, 62–88. [CrossRef]
149. Guarracino, I.; Mellor, A.; Ekins-Daukes, N.J.; Markides, C.N. Dynamic Coupled Thermal-and-Electrical Modelling of Sheet-and-Tube Hybrid Photovoltaic/Thermal (PVT) Collectors. *Appl. Therm. Eng.* **2016**, *101*, 778–795. [CrossRef]
150. HUANG, B.J.; LIN, T.H.; HUNG, W.C.; SUN, F.S. Performance evaluation of solar photovoltaic/thermal systems. *Dig. Liver Dis.* **2001**, *70*, 443–448. [CrossRef]
151. Li, G.; Pei, G.; Ji, J.; Su, Y. Outdoor Overall Performance of a Novel Air-Gap-Lens-Walled Compound Parabolic Concentrator (ALCPC) Incorporated with Photovoltaic/Thermal System. *Appl. Energy* **2015**, *144*, 214–223. [CrossRef]
152. Cappelletti, A.; Ceccherini Nelli, L.; Reatti, A. Integration and Architectural Issues of a Photovoltaic/Thermal Linear Solar Concentrator. *Sol. Energy* **2018**, *169*, 362–373. [CrossRef]
153. Lu, W.; Wu, Y.; Eames, P. Design and Development of a Building Façade Integrated Asymmetric Compound Parabolic Photovoltaic Concentrator (BFI-ACP-PV). *Appl. Energy* **2018**, *220*, 325–336. [CrossRef]
154. Lu, W.; Liu, Z.; Flor, J.F.; Wu, Y.; Yang, M. Investigation on Designed Fins-Enhanced Phase Change Materials System for Thermal Management of a Novel Building Integrated Concentrating PV. *Appl. Energy* **2018**, *225*, 696–709. [CrossRef]
155. Rahmanian, S.; Rahmanian-Koushkaki, H.; Omidvar, P.; Shahsavari, A. Nanofluid-PCM Heat Sink for Building Integrated Concentrated Photovoltaic with Thermal Energy Storage and Recovery Capability. *Sustain. Energy Technol. Assess.* **2021**, *46*, 101223. [CrossRef]
156. Mammo, E.D.; Sellami, N.; Mallick, T.K. Performance Analysis of a Reflective 3D Crossed Compound Parabolic Concentrating Photovoltaic System for Building Façade Integration. *Prog. Photovolt. Res. Appl.* **2012**, *21*, 1095–1103. [CrossRef]

157. Sellami, N.; Mallick, T.K. Optical Characterisation and Optimisation of a Static Window Integrated Concentrating Photovoltaic System. *Sol. Energy* **2013**, *91*, 273–282. [\[CrossRef\]](#)
158. Sabry, M.; Abdel-Hadi, Y.A.; Ghitas, A. PV-Integrated CPC for Transparent Façades. *Energy Build.* **2013**, *66*, 480–484. [\[CrossRef\]](#)
159. Tang, R.; Wang, J. A Note on Multiple Reflections of Radiation within CPCs and Its Effect on Calculations of Energy Collection. *Renew. Energy* **2013**, *57*, 490–496. [\[CrossRef\]](#)
160. Li, G.; Pei, G.; Ji, J.; Su, Y.; Zhou, H.; Cai, J. Structure Optimization and Annual Performance Analysis of the Lens-Walled Compound Parabolic Concentrator. *Int. J. Green Energy* **2015**, *13*, 944–950. [\[CrossRef\]](#)
161. Xuan, Q.; Li, G.; Pei, G.; Ji, J.; Su, Y.; Zhao, B. Optimization Design and Performance Analysis of a Novel Asymmetric Compound Parabolic Concentrator with Rotation Angle for Building Application. *Sol. Energy* **2017**, *158*, 808–818. [\[CrossRef\]](#)
162. Xuan, Q.; Li, G.; Lu, Y.; Zhao, X.; Su, Y.; Ji, J.; Pei, G. A General Optimization Strategy for the Annual Performance Enhancement of a Solar Concentrating System Incorporated in the South-Facing Wall of a Building. *Indoor Built Environ.* **2020**, *29*, 1386–1398. [\[CrossRef\]](#)
163. Xuan, Q.; Li, G.; Lu, Y.; Zhao, B.; Zhao, X.; Su, Y.; Ji, J.; Pei, G. Design, Optimization and Performance Analysis of an Asymmetric Concentrator-PV Type Window for the Building South Wall Application. *Sol. Energy* **2019**, *193*, 422–433. [\[CrossRef\]](#)
164. Li, J.; Zhang, W.; He, B.; Xie, L.; Hao, X.; Mallick, T.; Shanks, K.; Chen, M.; Li, Z. Experimental Study on the Comprehensive Performance of Building Curtain Wall Integrated Compound Parabolic Concentrating Photovoltaic. *Energy* **2021**, *227*, 120507. [\[CrossRef\]](#)
165. Liang, S.; Zheng, H.; Wang, X.; Ma, X.; Zhao, Z. Design and Performance Validation on a Solar Louver with Concentrating-Photovoltaic-Thermal Modules. *Renew. Energy* **2022**, *191*, 71–83. [\[CrossRef\]](#)
166. Barone, G.; Zacharopoulos, A.; Buonomano, A.; Forzano, C.; Giuzio, G.F.; Mondol, J.; Palombo, A.; Pugsley, A.; Smyth, M. Concentrating PhotoVoltaic Glazing (CoPVG) System: Modelling and Simulation of Smart Building Façade. *Energy* **2022**, *238*, 121597. [\[CrossRef\]](#)
167. Zarcone, R.; Brocato, M.; Bernardoni, P.; Vincenzi, D. Building Integrated Photovoltaic System for a Solar Infrastructure: Liv-Lib' Project. *Energy Procedia* **2016**, *91*, 887–896. [\[CrossRef\]](#)
168. Barone, G.; Buonomano, A.; Chang, R.; Forzano, C.; Giuzio, G.F.; Mondol, J.; Palombo, A.; Pugsley, A.; Smyth, M.; Zacharopoulos, A. Modelling and Simulation of Building Integrated Concentrating Photovoltaic/Thermal Glazing (CoPVTG) Systems: Comprehensive Energy and Economic Analysis. *Renew. Energy* **2022**, *193*, 1121–1131. [\[CrossRef\]](#)
169. Bernardoni, P.; Mangherini, G.; Gjestila, M.; Andreoli, A.; Vincenzi, D. Performance Optimization of Luminescent Solar Concentrators under Several Shading Conditions. *Energies* **2021**, *14*, 816. [\[CrossRef\]](#)
170. Tonezzer, M.; Gutierrez, D.; Vincenzi, D. Luminescent Solar Concentrators—State of the Art and Future Perspectives. In *Solar Cell Nanotechnology*; Scrivener Publishing LLC: Beverly, MA, USA, 2013; Chapter 12; pp. 293–315. [\[CrossRef\]](#)
171. Corrado, C.; Leow, S.W.; Osborn, M.; Chan, E.; Balaban, B.; Carter, S.A. Optimization of Gain and Energy Conversion Efficiency Using Front-Facing Photovoltaic Cell Luminescent Solar Concentrator Design. *Sol. Energy Mater. Sol. Cells* **2013**, *111*, 74–81. [\[CrossRef\]](#)
172. Buonomano, A.; Calise, F.; Palombo, A.; Vicidomini, M. Transient Analysis, Exergy and Thermo-Economic Modelling of Façade Integrated Photovoltaic/Thermal Solar Collectors. *Renew. Energy* **2019**, *137*, 109–126. [\[CrossRef\]](#)
173. Novelli, N.; Phillips, K.; Shultz, J.; Derby, M.M.; Salvias, R.; Craft, J.; Stark, P.; Jensen, M.; Derby, S.; Dyson, A. Experimental Investigation of a Building-Integrated, Transparent, Concentrating Photovoltaic and Thermal Collector. *Renew. Energy* **2021**, *176*, 617–634. [\[CrossRef\]](#)
174. Pugsley, A.; Zacharopoulos, A.; Mondol, J.D.; Smyth, M. BIPV/T Façades—A New Opportunity for Integrated Collector-Storage Solar Water Heaters? Part 2: Physical Realisation and Laboratory Testing. *Sol. Energy* **2020**, *206*, 751–769. [\[CrossRef\]](#)
175. Pereira, R.; Aelenei, L. Optimization Assessment of the Energy Performance of a BIPV/T-PCM System Using Genetic Algorithms. *Renew. Energy* **2019**, *137*, 157–166. [\[CrossRef\]](#)
176. Sohani, A.; Dehnavi, A.; Sayyaadi, H.; Hoseinzadeh, S.; Goodarzi, E.; Garcia, D.A.; Groppi, D. The Real-Time Dynamic Multi-Objective Optimization of a Building Integrated Photovoltaic Thermal (BIPV/T) System Enhanced by Phase Change Materials. *J. Energy Storage* **2022**, *46*, 103777. [\[CrossRef\]](#)
177. Kim, J.H.; Yu, J.S.; Gaucher-loksts, E.; Roy, B.; Delisle, V.; Kim, J.T. Performance Assessment of an Air-Type BIPVT Collector with Perforated Baffles through Indoor and Outdoor Experiments. *Energies* **2022**, *15*, 3779. [\[CrossRef\]](#)
178. Hami, K.; Draoui, B.; Hami, O. The Thermal Performances of a Solar Wall. *Energy* **2012**, *39*, 11–16. [\[CrossRef\]](#)
179. Duan, S.; Jing, C.; Zhao, Z. Energy and Exergy Analysis of Different Trombe Walls. *Energy Build.* **2016**, *126*, 517–523. [\[CrossRef\]](#)
180. Ke, W.; Ji, J.; Zhang, C.; Xie, H.; Tang, Y.; Wang, C. Effects of the PCM Layer Position on the Comprehensive Performance of a Built-Middle PV-Trombe Wall System for Building Application in the Heating Season. *Energy* **2023**, *267*, 126562. [\[CrossRef\]](#)
181. Abed, A.A.; Ahmed, O.K.; Weis, M.M.; Hamada, K.I. Performance Augmentation of a PV/Trombe Wall Using Al₂O₃/Water Nano-Fluid: An Experimental Investigation. *Renew. Energy* **2020**, *157*, 515–529. [\[CrossRef\]](#)
182. Ahmed, O.K.; Hamada, K.I.; Salih, A.M. Enhancement of the Performance of Photovoltaic/Trombe Wall System Using the Porous Medium: Experimental and Theoretical Study. *Energy* **2019**, *171*, 14–26. [\[CrossRef\]](#)
183. Park, K.E.; Kang, G.H.; Kim, H.I.; Yu, G.J.; Kim, J.T. Analysis of Thermal and Electrical Performance of Semi-Transparent Photovoltaic (PV) Module. *Energy* **2010**, *35*, 2681–2687. [\[CrossRef\]](#)

184. Lu, L.; Law, K.M. Overall Energy Performance of Semi-Transparent Single-Glazed Photovoltaic (PV) Window for a Typical Office in Hong Kong. *Renew. Energy* **2013**, *49*, 250–254. [[CrossRef](#)]
185. Miyazaki, T.; Akisawa, A.; Kashiwagi, T. Energy Savings of Office Buildings by the Use of Semi-Transparent Solar Cells for Windows. *Renew. Energy* **2005**, *30*, 281–304. [[CrossRef](#)]
186. He, W.; Zhang, Y.X.; Sun, W.; Hou, J.X.; Jiang, Q.Y.; Ji, J. Experimental and Numerical Investigation on the Performance of Amorphous Silicon Photovoltaics Window in East China. *Build. Environ.* **2011**, *46*, 363–369. [[CrossRef](#)]
187. Liao, W.; Xu, S. Energy Performance Comparison among See-through Amorphous-Silicon PV (Photovoltaic) Glazings and Traditional Glazings under Different Architectural Conditions in China. *Energy* **2015**, *83*, 267–275. [[CrossRef](#)]
188. Chae, Y.T.; Kim, J.; Park, H.; Shin, B. Building Energy Performance Evaluation of Building Integrated Photovoltaic (BIPV) Window with Semi-Transparent Solar Cells. *Appl. Energy* **2014**, *129*, 217–227. [[CrossRef](#)]
189. Zhang, W.; Lu, L.; Peng, J.; Song, A. Comparison of the Overall Energy Performance of Semi-Transparent Photovoltaic Windows and Common Energy-Efficient Windows in Hong Kong. *Energy Build.* **2016**, *128*, 511–518. [[CrossRef](#)]
190. Chow, T.T.; Fong, K.F.; He, W.; Lin, Z.; Chan, A.L.S. Performance Evaluation of a PV Ventilated Window Applying to Office Building of Hong Kong. *Energy Build.* **2007**, *39*, 643–650. [[CrossRef](#)]
191. Barman, S.; Chowdhury, A.; Mathur, S.; Mathur, J. Assessment of the Efficiency of Window Integrated CdTe Based Semi-Transparent Photovoltaic Module. *Sustain. Cities Soc.* **2018**, *37*, 250–262. [[CrossRef](#)]
192. Meng, W.; Jinqing, P.; Hongxing, Y.; Yimo, L. Performance Evaluation of Semi-Transparent CdTe Thin Film PV Window Applying on Commercial Buildings in Hong Kong. *Energy Procedia* **2018**, *152*, 1091–1096. [[CrossRef](#)]
193. Alrashidi, H.; Ghosh, A.; Issa, W.; Sellami, N.; Mallick, T.K.; Sundaram, S. Evaluation of Solar Factor Using Spectral Analysis for CdTe Photovoltaic Glazing. *Mater. Lett.* **2019**, *237*, 332–335. [[CrossRef](#)]
194. Kang, J.G.; Kim, J.H.; Kim, J.T. Performance Evaluation of DSC Windows for Buildings. *Int. J. Photoenergy* **2013**, *2013*, 472086. [[CrossRef](#)]
195. Yoon, S.; Tak, S.; Kim, J.; Jun, Y.; Kang, K.; Park, J. Application of Transparent Dye-Sensitized Solar Cells to Building Integrated Photovoltaic Systems. *Build. Environ.* **2011**, *46*, 1899–1904. [[CrossRef](#)]
196. Morini, M.; Corrao, R. Energy Optimization of BIPV Glass Blocks: A Multi-Software Study. *Energy Procedia* **2017**, *111*, 982–992. [[CrossRef](#)]
197. Selvaraj, P.; Ghosh, A.; Mallick, T.K.; Sundaram, S. Investigation of Semi-Transparent Dye-Sensitized Solar Cells for Fenestration Integration. *Renew. Energy* **2019**, *141*, 516–525. [[CrossRef](#)]
198. Roy, A.; Ghosh, A.; Bhandari, S.; Selvaraj, P.; Sundaram, S.; Mallick, T.K. Color Comfort Evaluation of Dye-Sensitized Solar Cell (DSSC) Based Building-Integrated Photovoltaic (BIPV) Glazing after 2 Years of Ambient Exposure. *J. Phys. Chem. C* **2019**, *123*, 23834–23837. [[CrossRef](#)]
199. Tong, G.; Son, D.Y.; Ono, L.K.; Liu, Y.; Hu, Y.; Zhang, H.; Jamshaid, A.; Qiu, L.; Liu, Z.; Qi, Y. Scalable Fabrication of >90 Cm² Perovskite Solar Modules with >1000 h Operational Stability Based on the Intermediate Phase Strategy. *Adv. Energy Mater.* **2021**, *11*, 2003712. [[CrossRef](#)]
200. Ghosh, A.; Bhandari, S.; Sundaram, S.; Mallick, T.K. Carbon Counter Electrode Mesoscopic Ambient Processed & Characterised Perovskite for Adaptive BIPV Fenestration. *Renew. Energy* **2020**, *145*, 2151–2158. [[CrossRef](#)]
201. Bhandari, S.; Ghosh, A.; Roy, A.; Mallick, T.K.; Sundaram, S. Compelling Temperature Behaviour of Carbon-Perovskite Solar Cell for Fenestration at Various Climates. *Chem. Eng. J. Adv.* **2022**, *10*, 100267. [[CrossRef](#)]
202. Alrashidi, H.; Issa, W.; Sellami, N.; Sundaram, S.; Mallick, T. Thermal Performance Evaluation and Energy Saving Potential of Semi-Transparent CdTe in Façade BIPV. *Sol. Energy* **2022**, *232*, 84–91. [[CrossRef](#)]
203. Yu, J.C.; Sun, J.; Chandrasekaran, N.; Dunn, C.J.; Chesman, A.S.R.; Jasieniak, J.J. Semi-Transparent Perovskite Solar Cells with a Cross-Linked Hole Transport Layer. *Nano Energy* **2020**, *71*, 104635. [[CrossRef](#)]
204. Fraunhofer ISE. Institute for Solar Energy Systems Photovoltaic Report. Available online: <https://www.ise.fraunhofer.de/content/dam/ise/de/documents/publications/studies/Photovoltaics-Report.pdf> (accessed on 24 July 2023).
205. Masson, G.; Kaizuka, I. Trends in PV Applications 2022. 2022. Available online: https://iea-pvps.org/wp-content/uploads/2023/02/PVPS_Trend_Report_2022.pdf (accessed on 13 July 2023).
206. Europe, S. Solar Skins: An Opportunity for Greener Cities. Available online: <https://etip-pv.eu/publications/etip-pv-publications/download/solar-skins-an-opportunity-for-greener-cities> (accessed on 3 August 2023).
207. Sarkar, D.; Kumar, A.; Sadhu, P.K. A Survey on Development and Recent Trends of Renewable Energy Generation from BIPV Systems. *IETE Tech. Rev. (Inst. Electron. Telecommun. Eng. India)* **2020**, *37*, 258–280. [[CrossRef](#)]
208. Alim, M.A.; Tao, Z.; Hassan, M.K.; Rahman, A.; Wang, B.; Zhang, C.; Samali, B. Is It Time to Embrace Building Integrated Photovoltaics? A Review with Particular Focus on Australia. *Sol. Energy* **2019**, *188*, 1118–1133. [[CrossRef](#)]
209. Agathokleous, R.A.; Kalogirou, S.A. Status, Barriers and Perspectives of Building Integrated Photovoltaic Systems. *Energy* **2020**, *191*, 116471. [[CrossRef](#)]
210. Skandalos, N.; Wang, M.; Kapsalis, V.; D’Agostino, D.; Parker, D.; Bhuvad, S.S.; Udayraj; Peng, J.; Karamanis, D. Building PV Integration According to Regional Climate Conditions: BIPV Regional Adaptability Extending Köppen-Geiger Climate Classification against Urban and Climate-Related Temperature Increases. *Renew. Sustain. Energy Rev.* **2022**, *169*, 112950. [[CrossRef](#)]

211. Yang, R.; Zang, Y.; Yang, J.; Wakefield, R.; Nguyen, K.; Shi, L.; Trigunaryah, B.; Parolini, F.; Bonomo, P.; Frontini, F.; et al. Fire Safety Requirements for Building Integrated Photovoltaics (BIPV): A Cross-Country Comparison. *Renew. Sustain. Energy Rev.* **2023**, *173*, 113112. [[CrossRef](#)]
212. Borrebæk, P.O.A.; Jelle, B.P.; Zhang, Z. Avoiding Snow and Ice Accretion on Building Integrated Photovoltaics—Challenges, Strategies, and Opportunities. *Sol. Energy Mater. Sol. Cells* **2020**, *206*, 110306. [[CrossRef](#)]
213. Ghosh, A. Soiling Losses: A Barrier for India's Energy Security Dependency from Photovoltaic Power. *Challenges* **2020**, *11*, 9. [[CrossRef](#)]
214. Nundy, S.; Ghosh, A.; Mallick, T.K. Hydrophilic and Superhydrophilic Self-Cleaning Coatings by Morphologically Varying ZnO Microstructures for Photovoltaic and Glazing Applications. *ACS Omega* **2020**, *5*, 1033–1039. [[CrossRef](#)] [[PubMed](#)]
215. Nundy, S.; Ghosh, A.; Tahir, A.; Mallick, T.K. Role of Hafnium Doping on Wetting Transition Tuning the Wettability Properties of ZnO and Doped Thin Films: Self-Cleaning Coating for Solar Application. *ACS Appl. Mater. Interfaces* **2021**, *13*, 25540–25552. [[CrossRef](#)] [[PubMed](#)]
216. Kou, Z.; Wang, J.; Tong, X.; Lei, P.; Gao, Y.; Zhang, S.; Cui, X.; Wu, S.; Cai, G. Multi-Functional Electrochromic Energy Storage Smart Window Powered by CZTSSe Solar Cell for Intelligent Managing Solar Radiation of Building. *Sol. Energy Mater. Sol. Cells* **2023**, *254*, 112273. [[CrossRef](#)]

Disclaimer/Publisher's Note: The statements, opinions and data contained in all publications are solely those of the individual author(s) and contributor(s) and not of MDPI and/or the editor(s). MDPI and/or the editor(s) disclaim responsibility for any injury to people or property resulting from any ideas, methods, instructions or products referred to in the content.